Ice Damage to Concrete

Erland M. Schulson

April 1998

Abstract: Concrete is a porous material. When saturated with water and then cooled to below 0°C, it cracks internally. Upon repeated freezing and thawing, the cracks grow, interact, and lead eventually to macroscopic degradation, termed ice damage. This report reviews the phenomenon and considers the underlying mechanisms. New explanations are given for the deleterious effect of deicer salts and for the beneficial effect of entrained air.

Special Report 98-6

**US Army Corps
of Engineers**®
Cold Regions Research &
Engineering Laboratory

Ice Damage to Concrete

Erland M. Schulson

April 1998

PREFACE

The contents of this report are not be used for advertising or promotional purposes. Citation of brand names does not constitute an official endorsement or approval of the use of such commercial products.

CONTENTS

ILLUSTRATIONS

TABLES

Ice Damage to Concrete

ERLAND M. SCHULSON

INTRODUCTION

Although perhaps the oldest engineered material and certainly one of the most used and studied, concrete continues to challenge the imagination. At stake is service life. Owing to its porous microstructure, the material is vulnerable to environmental degradation. Corrosion of steel reinforcement bars, alkali-silica reactions, sulfate attack, and thermal cycling below the bulk freezing point of water all lead to expansive products that damage the interior and shorten life. The cost is huge. For instance, the Federal Highway Administration estimates (FHWA 1995) that the annual cost to maintain the nation's highways and bridges, many of which are made from concrete, is $54.8 billion. The estimate to improve the system over 20 years is $1.5 trillion. The positive view is that small improvements in materials performance will lead to major savings.

The challenge, then, is to the materials scientist and might be stated as follows: design an easily castable/formable cementitious material whose price, properties, and availability are essentially the same as today's concrete and whose durability is significantly greater, with no adverse effects on the environment. This is tantamount to designing a material in which the degradation processes are eliminated, or at least suppressed. The issue thus reduces to the elucidation and control of the mechanisms underlying the various processes.

It is here that the limitations in understanding are met. Concrete, as discussed below, is an extraordinarily complex material. It is very difficult to vary one microstructural element independent of the others. As a result, structure–property relationships remain elusive.

This report reviews the problem of ice damage to concrete, or more explicitly the internal cracking that accompanies the freezing of water within its pores, often in the presence of deicing salts. (The term "ice damage" is introduced to include both frost damage and scaling in the presence of to deicer salts.) The report first addresses the structure of the material, and describes (in three appendices by I. Baker) the techniques that have been used to reveal the microstructure. It then considers the factors that affect ice damage. Finally, it considers the underlying mechanisms.

THE STRUCTURE OF CONCRETE

Concrete, when fully hardened, contains a variety of microstructural features on a variety of scales. To the unaided eye, it appears from a polished section to be essentially a two-phase composite—a matrix of hardened mortar plus coarse (> 5-mm) aggregate that occupies about 75% of its volume. Dissolved air may also be detected, as coarse spherical pores distributed throughout the matrix. On a somewhat finer scale, the mortar itself appears as a two-phase composite of hardened/hydrated cement paste plus fine aggregate or sand. At a finer scale still, the hydrated cement paste is seen to be a multiphase composite, consisting typically of about 10–15% (by vol.) clinker or unhydrated cement globules (mainly a mixture of impure C_3S*, termed alite, plus impure C_2S, termed belite), about 20% of plate-like CH, and about 30% porosity, all dispersed within a matrix of C-S-H. The pores are the remnants of the sites which held the water required for hydration. They are finer than air bubbles, have irregular shapes, and are interconnected. At a still finer scale, even tinier pores are detected within the C-S-H and constitute about 28% of its volume (Powers and Brownyard 1947). The C-S-H matrix and the porosity are the most important elements relevant to ice damage.

C-S-H

Although still under active investigation (e.g., Taylor 1986, 1992, Allan et al. 1987, Pope et al. 1992, Bergstrom 1992, Christensen et al. 1994, Jennings and Tennis 1994, Tarrida et al. 1995, Meredith et al. 1995, Hall et al. 1995, Gu and Beaudoin 1996, Viehland et al. 1996) certain characteristics of C-S-

*We adopt the cement chemist's nomenclature. Accordingly, C = CaO, S = SiO_2, H = H_2O, A = Al_2O_3 and F = Fe_2O_3.

H have been established. Unlike the other solid constituents of the microstructure, the material is only partially crystalline. It is a disordered, layered substance (Taylor 1986, 1992) comprising structurally imperfect derivatives of jennite ($C_9S_6H_{11}$) and 1.4-nm tobermorite ($C_5S_6H_9$). The crystalline content is on the nanometer scale (about 5 nm) and is dispersed within an amorphous matrix within which some short-range ordered regions are also dispersed (Viehland et al. 1996) The water is bound between the layers. C-S-H is often considered to be gel-like (i.e., nearly amorphous) and so its pores are termed *gel pores.* Its Ca/Si ratio varies from 1.7 to 2.0 (Taylor 1986), although this appears to vary on the submicron scale (Viehland et al. 1996) and to be closer to about 1.8 in fully hydrated cement.

C-S-H consists of inner and outer products, at least when made from C_3S and water alone (Groves 1985). The inner material is the product of hydration, which forms within the original boundaries of the parent C_3S particle. The outer product forms more or less beyond the original boundaries (although some also forms within the original boundaries) and consists of CH flakes, larger capillary pores, and lath-like C-S-H. Sometimes within the outer product acicular C-S-H is seen, which could actually be rolled up foils. Both inner and outer products are porous, although the inner product is thought to be less so*. Barring the spatial variation in Ca/Si ratio, both products appear to have about the same average Ca/Si ratio, i.e., 1.7 in Groves' (1985) material. Interestingly, rupture appears to occur just inside the inner/outer interface, not at the C-S-H/CH boundary, suggesting that the negative view of the plate-like phase in relation to strength and fracture may not be justified (Groves 1985). As far as ice damage is concerned, one wonders whether the outer product is the more important.

At the molecular level C-S-H consists of polysilicate anions. The basic unit or monomer is the SiO_4^{-4} tetrahedon: Si occupies the center and bonds with four oxygen atoms. The polymer is formed by the tetrahedra linking together, as in silicate minerals. The Ca^{++}ions are incorporated in a manner that preserves electrical neutrality. This implies that in Si_2O_7 dimers and in Si_3O_{10} trimers, for instance, there are three and four such ions, respectively, and that the Ca/Si ratios, respec-

tively, are 1.5 and 1.33. Water molecules terminate the chains but do not affect the charge balance. Should Ca/Si exceed 1.5 in dimeric C-S-H or exceed 1.33 in trimeric material, hydroxil ions or other negative ions would probably be incorporated within the gel to preserve its electrical neutrality. The degree of polymerization is around two to three in ordinary hardened cement and increases to about four as the water/cement (w/c) ratio[†] decreases, as evident from studies using solid state ^{29}Si nuclear magnetic resonance spectroscopy (Sellevold et al. 1994, Justnes et al. 1990, 1992). It also increases upon the addition of silica fume (see *Silica Fume*). The higher degree expels water, which then participates in the hydration reaction.

The degree of polymerization may control the strength of C-S-H, just as it governs the strength of carbonaceous polymers, although this point has not been established. In keeping with it, however, is the strengthening which accompanies both the reduction in w/c and the addition of silica fume (Mehta and Montiero 1993). In natural silicate minerals, SiO_4^{-4} tetradedra are linked together in various ways, depending upon the metal ion concentration. For instance, when combined with metal oxides like CaO, MgO and Al_2O_3, the degree of polymerization increases with decreasing amounts of metal (Ashby and Jones 1986) and the structures that form depend upon how the oxygen atoms are shared: chains from the sharing of two oxygens between tetrahedra, sheets from the sharing of three oxygens, and networks from the sharing of four. If C-S-H exhibits similar behavior, then perhaps a variety of morphologies (stringy, filmy, and networky) develop depending upon the local chemistry, i.e., on whether the C-S-H formed from the hydration of alite (impure C_3S), or belite (impure C_2S) and whether the other primary constituents of portland cement, C_3A and C_4AF, participated.

Porosity

The pores are important because they hold the water that freezes upon cooling. In this sense, hardened portland cement is analogous to soil. The difference is that soils are composed of discrete particles that contact at isolated points. Hardened cement, on the other hand, like sedimentary rock (Jaegar and Cook 1979), is better viewed as a solid

---

*Personal communication, H. M. Jennings, Northwestern University, 1996.

[†]In keeping with standard practice w/c defines the ratio of the weight of water to the weight of cement.

Table 1. Calculated porosities from Powers-Brownyard (1947) model (Taylor 1992).

w/c ratio	Fraction of cement hydrated	Capillary porosity	Gel porosity	Total water porosity
0.3	0.00	0.49	0.00	0.49
0.3	0.79	0.00	0.27	0.27
0.4	0.00	0.56	0.00	0.56
0.4	1.00	0.03	0.29	0.32
0.5	0.00	0.61	0.00	0.61
0.5	1.00	0.15	0.26	0.41
0.6	0.00	0.65	0.00	0.65
0.6	1.00	0.24	0.23	0.47

skeleton traversed by a more or less interconnected network of pores. The pore volume (capillary plus gel pores, but excluding air pores) is governed mainly by the w/c ratio. For instance, the pore volume fraction within fully hydrated portland cement decreases from around 0.5 at w/c = 0.6 (Table 1), to about 0.3 at w/c = 0.3–0.4 (Powers and Brownyard 1947). The pores within the driest cement (w/c = 0.3) are essentially of the gel type only.

It is necessary to consider not only pore size, but also area, size distribution, shape, roughness, and connectivity (Smith et al. 1994). Measurement of these characteristics is not easy (Taylor 1992) and is discussed at length in Appendix A. Assessments are commonly based upon the penetration of the pore system by fluids, and so depend upon the characteristics of the penetrant as well. For instance, owing possibly to differences in size (Rarick et al. 1995), nitrogen (0.44 nm), and other nonpolar sorbates are less penetrating than water (0.39 nm) and so give lower measures of surface area (Jennings 1996*; also see Taylor 1992). The examination may alter the structure, both during the pretreatments to drive off adsorbed water and during the penetration. For instance, drying 6-month-old portland cement (w/c = 0.4) for one week at 105°C after storing at 100% relative humidity increases significantly its bulk resistivity after rewetting (Christensen et al. 1994). Jennings (1996) finds that the use of mercury as a penetrant damages the pore structure owing to the high pres-

sure needed for penetrating small spaces. Other concerns include the restriction to entry of the penetrant by the neck of the pore and the effect this has on its apparent size. Wettability is also an issue and is particularly relevant to the use of mercury intrusion porosimetry: the wetting angle there is assumed to be about 130°–140° (Good 1984). Importantly, it is the cosine of this angle to which the size is related, and so uncertainty here leads to uncertainty in the pore size distribution. Moreover, assessments by gas adsorption and fluid penetration alone seem to ignore the possibility that the pores may not be truly Euclidian objects, but rather part of a fractal structure (Allan et al. 1987). In such a case, nuclear magnetic resonance spectroscopy and scattering methods (Smith et al. 1994) such as neutron scattering[†] would help to obtain a more complete picture. The net result is that the pore structure is not completely resolved.

Nevertheless, several points are clear. The internal surface area of fully hardened portland cement is relatively large. From adsorption measurements using water vapor, Powers and Brownyard (1947) obtained a value of 175 m^2/g. The area is now considered to be around 200 m^2/g (Rarick et al. 1995). It is also clear that the size distribution within well cured pastes is quite broad, ranging mainly from around 3 to 100 nm (Taylor 1992) (Fig. 1), the gel pores being the smallest ones. The range extends to about 1000 nm or larger in young pastes and to 1 mm or more when air bubbles are in-

*Personal communication, H. M. Jennings, Northwestern University, 1996.

[†]Personal communication, R.A. Livingston, Federal Highway Administration, 1996.
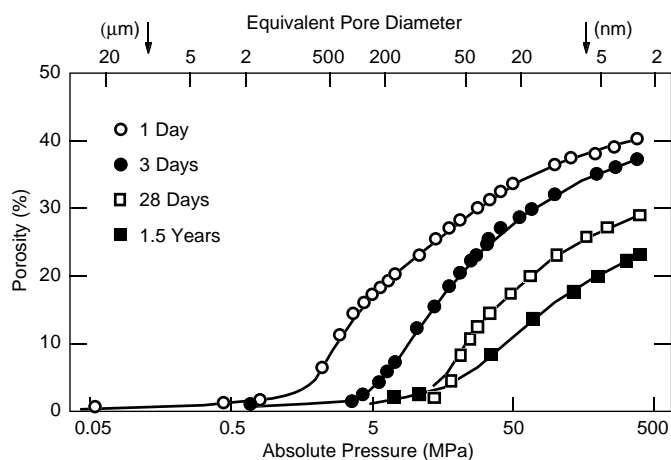
Figure 1. Pore sizes in portland cement (Feldman 1981, from Taylor 1992).

cluded. Reductions in the w/c ratio shift the distribution to finer sizes, owing to a reduction in the number density of capillary pores (Parrott 1989). The fraction above 4 nm, for instance, decreases from 0.26 to 0.07 upon reducing w/c from 0.65 to 0.35 (Parrott 1986).

Pores are often classified by their diameter ϕ using nomenclature of the International Union of Pure and Applied Chemists (Gregg et al. 1982, Sing et al. 1985): micropores ($\phi < 2$ nm), mesopores ($2 < \phi < 50$ nm), or macropores ($\phi > 50$ nm). This classification is rather artificial, because it is based more on limitations of technique than on physical and chemical characteristics.

Imagining the pore structure is a challenge. One image is of a bundle of roughened grapes, the grapes themselves being C-S-H nodules about 5 nm in diameter (Allan et al. 1987) and the spaces between, the pores. This image suggests somewhat cuspy holes of different sizes with rough surfaces, interconnected at their necks. A variation is to imagine not only linear or string-like bundles, but also plate or foil-like arrays. Another picture, as already implied, is of unfilled spaces within a mixture of strings, films, and networks. The more Euclidean model is the easier to imagine and so is the one adopted here.

Interfacial transition zone

Although implied, the cement binder is not necessarily homogeneous. Instead, in at least some concretes, it exhibits gradients within the vicinity of the aggregate/matrix interface: gradations in porosity, in portlandite (CH) and in anhydrous cement. In other words, the microstructure of the paste near the aggregate appears to differ from that within the bulk (Taylor 1992). In fact, an interfacial transition zone (ITZ) has been identified by some writers (e.g., Mehta and Montiero 1993) as a distinct phase to which separate properties are given. That the interfacial region may be significant is evident from the fact that the particles of aggregate are separated by rather small distances, implying that a large fraction of the interparticle volume may be composed of microstructural gradients.

The ITZ is thought to be a shell-like region, about 30–50 μm thick, which surrounds the aggregate particles (Farran 1956, Hadley 1972, Barnes 1978, Ollivier et al. 1980, Monteiro and Mehta 1985, Scrivener and Gartner 1988). Within the zones, the levels of porosity and of portlandite are considered to be higher than in the matrix; the anhydrous cement, to be lower. The current view is that, while controversial, the ITZ appears to be a feature whose character depends on the details of materials processing, such as the degree of shearing at the particle/aggregate interface during setting. To better appreciate the feature a nondestructive method of characterization is needed.

That the ITZ is real in at least some concretes is supported by two recent observations. Using scanning acoustic microscopy, Prasad et al. (1996) observed interfacial features that are similar in size (around 50 μm thick) to those noted by Monteiro and Mehta (1985) and by Scrivener and Gartner (1988). And Tan (1995) found the specific fracture energy of interfaces in sandstone mortar (14 J/m^2) and limestone mortar (6 J/m^2) to be much lower than that of the mortar itself (80 J/m^2). Also, he

4

noted that when aggregate was positioned well below the root of a notch, decohesion was initiated not at the root, where the tensile stress was highest, but at the aggregate/mortar interface.

Whether the ITZ plays a role in ice damage is not clear. The attendant porosity, however, suggests that it could, for the spaces are probably filled with water when concrete is fully saturated.

Experimental techniques

Only a few experimental methods have been mentioned in the above discussion. In fact, many different techniques have been used to examine the microstructure. These are described and discussed in Appendices A–C. Small angle neutron scattering and environmental scanning electron microscopy are particularly worth noting. The former method provides information on the spatial array; the latter method offers the possibilities of diffraction analysis and chemical analysis using energy dispersion spectroscopy, techniques which have not yet been exploited. Other methods not yet applied to concrete are also discussed.

A complete picture of the microstructure will require the application of advanced techniques to reveal both the temporal and its spatial character.

ICE DAMAGE: THE FACTORS

Given that concrete is a porous material, it is not surprising that water, if not there initially, can enter during service and generate disruptive pressures upon freezing. Damage so generated is termed ice damage. It is initiated through the nucleation, growth, and interaction of microcracks. These processes usually occur internally. They are manifested by volume expansion during cooling (Powers and Helmuth 1953, Beaudoin and MacInis 1974) and by macroscopic cracks that develop after repeated cycles of freezing and thawing. The damage is exacerbated by deicing salts, which lead to spalling or scaling of the surface. Concrete pavements, bridge decks, bridge piers, runways, sidewalks, and water supply systems, for instance, are all vulnerable. Susceptibility is usually assessed using a standard laboratory test: ASTM C 666 measures residual dynamic modulus of elasticity; ASTM C 671 measures dilatation; and ASTM C 672 and the Swedish Standard SS 13 72 44 measure the scaling resistance of a horizontal surface in the presence of deicing salts or other chemicals (Pigeon and Pleau 1995). Several factors are important.

Water/cement ratio

A major factor is the w/c (water/cement) ratio. It determines not only the total capillary porosity (Powers and Brownyard 1947), but also the pore size distribution (e.g., Parrott 1989). As already noted, the lower the ratio, the lower is the porosity and the fewer are the larger pores within well cured cement, implying a lower maximum potential water content. Also, the permeability is lower, implying greater difficulty for water to enter the paste. Correspondingly, the resistance to freeze–thaw damage is greater (Verbeck and Landgren 1960, Marchand et al. 1995, Pigeon and Pleau 1995, Thorpe 1996).

The w/c effect is often coupled with a second one, namely the spacing of air bubbles (see next section), and then quantified in terms of a critical spacing L_c below which ice damage, or at least the rate of damage, is suppressed. For instance, Okada et al. (1981) subjected different concretes to 300 cycles of rapid freezing in water according to ASTM C 666(A) and found that the resistance increased (i.e., L_c increased) for w/c < 0.4 (Fig. 2). Kobayashi et al. (1981) and Pigeon (1989) obtained similar results. At low w/c ratios (<0.3) concrete apparently becomes immune (Gagne et al. 1990). Further work, in which the ASTM C 666(A) test coupled with pulse velocity and length change was used to evaluate 17 high-strength concretes, suggests that the critical w/c ratio may be somewhat greater than 0.3 in some mixes, but around 0.25 or lower in others (Pigeon and Langlois 1991), depending upon the fineness of the cement (more below) and upon the length of curing. Both factors influence the pore structure and thus the water content.

The w/c effect offers a way not only for lessening the vulnerability to ice damage, but also for raising strength. The latter property also increases as the porosity decreases (Kendall et al. 1983).

Entrained air

Entrained air is another major factor. When intentionally incorporated to around 5–7% of the volume of the concrete and appropriately distributed, ice damage can be greatly suppressed (e.g., Powers 1949, Powers and Helmuth 1953, Pigeon and Pleau 1995). Lower values are ineffective and higher levels weaken the material too much. The bubbles are actually incorporated within the cement binder and of that phase represent about 15–20% of its volume (Mindess and Young 1981). They are globular in shape, range in size from about 1 μm to 1 mm (although most fall within the range

Figure 2. Air-void spacing vs. w/c ratio for concrete mixtures subjected to 300 rapid freezing and thawing cycles (Okada et al. 1981, from Pigeon and Pleau 1995).
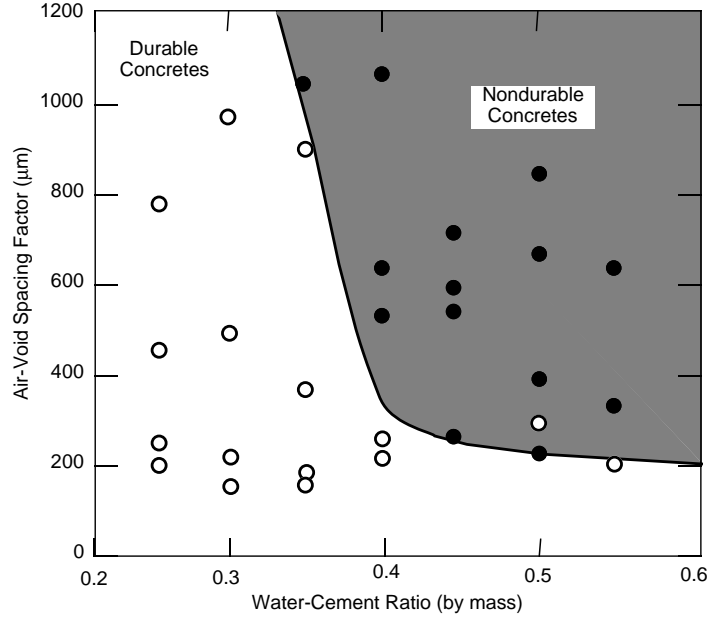
10–100 μm) and are spaced around 100 μm at the concentration noted (Pigeon and Pleau 1995). Air entrainment is now standard practice in cold climates. Whether it will continue to be for high performance/high strength concretes is an open question (El-Korchy et al. 1995), for the low w/c ratio may impart sufficient protection without the risk of weakening the material. While it may turn out to be more cost effective to produce durable concrete using an appropriate dispersion of air bubbles than by lowering the w/c ratio, as Thorpe

(1996) suggests, this practice would be at the expense of strength.

Air is entrained through the addition to the parent mix of small amounts (e.g., 0.2 to 1.0 mL/kg cement) of various chemicals, such as alkyl-benzyl sulphonates and salts of fatty acids, wood resin, and sulphonated hydrocarbons. These chemicals are surfactants that cause the mixing water to foam by lowering the air/water surface tension. The effect is to stabilize air bubbles, which then become entrained within the paste during mixing.
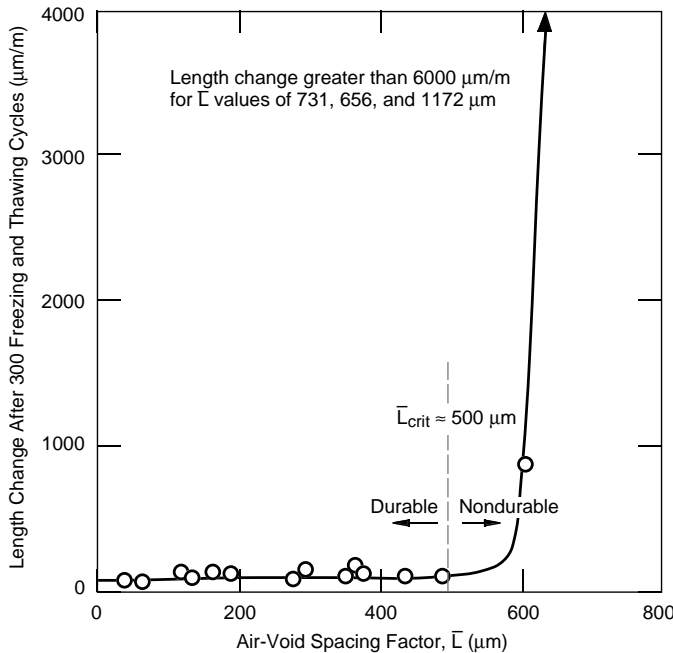

Figure 3. Length change vs. air-void spacing showing a critical spacing factor (Pigeon et al. 1986, from Marchand et al. 1995).

The resistance to ice damage is usually related to the spacing between the bubbles. Figure 3 illustrates this point where the resistance is expressed in terms of the increase in specimen length that arises from internal cracking. The data were obtained by Pigeon et al. (1986) from a systematic study of one concrete of w/c = 0.5 made from portland cement of one fine aggregate, one coarse (limestone) aggregate, and one curing procedure (14 days in water at 23°C), cycled in water 300 times between 5° and –18°C at 8°C/hr in accord with ASTM C 666(A). The resistance remained high until the average bubble spacing reached about 500 μm, above which it fell rapidly. Other studies show a similar effect, as reviewed by Pigeon and Pleau (1995). The spacing which marks the transition from durability to nondurability is termed the critical spacing factor L_c. Values recommended for concrete design are around L_c = 200 to 250 μm (Powers 1949, Backstrom et al. 1958). The average size of bubble is usually specified in terms of a specific surface area of around about 230 cm^2/cm^3 (Thorpe 1996). These specifications translate roughly to about 250×10^3 bubbles/cm^3 of around 100-μm diameter in cement paste whose air fraction by volume is between 0.15 and 0.2.

Not all investigators accept the idea of a clear relationship between ice damage and the bubble spacing (Mielenz 1968, Gjorv et al. 1978, Mather 1978). A possible resolution may be found in work by Litvan (1983). He observed that the volume of intermediate-sized (0.35- to 2-μm) pores, equivalent to the largest capillary pores, was higher within air-entrained concrete than within plain material. The beneficial effect, he suggested, may relate to these smaller features and not to the larger (typically 10- to 100-μm) air bubbles.

Even when air bubbles are present in sufficient number and in the appropriate distribution, internal cracking still occurs. Presumably, the critical spacing factor depends on the number of cycles and on the minimum temperature.

Degree of saturation

In the laboratory, material is usually fully saturated before being cycled. In the field, however, it may not be, depending on the availability of water, say as humidity in the atmosphere, and on the time available for ab/desorbing it. In other words, in practical situations, concrete may be less than fully saturated. For instance, the degree of saturation of concrete pavements in this country ranges between about 0.8 and 0.95 (Vanderhorst and Janssen 1990). It turns out that ice damage is not a problem when the degree of saturation is sufficiently low, even for non-air-entrained concrete (MacInnis and Beaudoin 1968, Litvan 1972b). The degree of saturation is thus another major factor.

Fagerlund (1971), Litvan (1973), and Enustun et al. (1994) have studied this point. The degree of saturation S is defined as the ratio of the weight of evaporable water (including the gel water) within the material at the time of freezing divided by the weight of evaporable water at complete saturation from the oven-dried (at 50°C) state to a state of constant weight under vacuum. From a series of experiments performed on non-air-entrained concrete of w/c around 0.4 to 0.5, Fagerlund (1977) concluded that the critical degree of saturation S_c is about 0.8 (Fig. 4). The S_c value in these experiments was obtained from measurements of the dynamic Young's modulus normalized with respect to the undamaged modu-
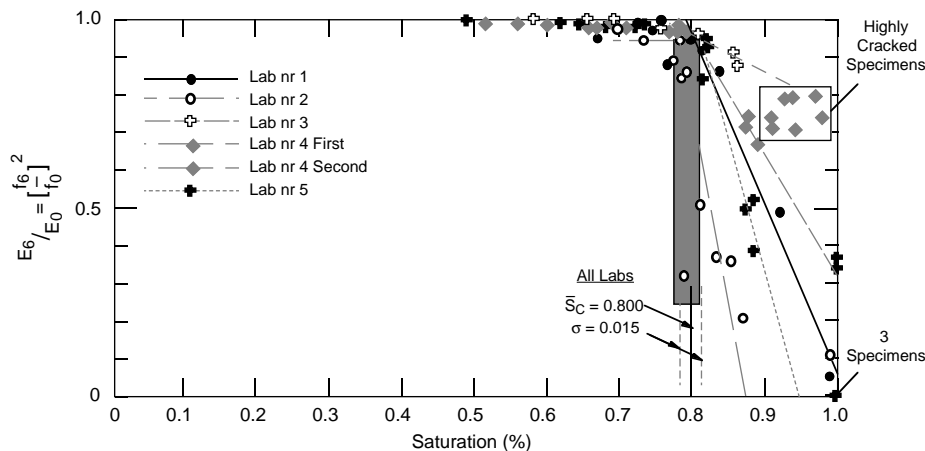

Figure 4. Dynamic Young's modulus (normalized) vs. degree of saturation for concrete measured in five different laboratories (Fagerlund 1977).

lus, following six freeze–thaw cycles to –18° or –20°C at a rate of 2° to 4° C/h. The actual value varies somewhat from one concrete to another, reflecting variations in the microstructure.

Note that the period of ice-immunity is governed by the kinetics of water absorption, and this is inversely related to the size of the pores. Thus, concretes containing smaller pores more quickly become saturated. Absorption kinetics also depend on the concentration of the water available, and has been considered by Fagerlund (1977). Note, too, that the specific value obtained for S_c reflects a specific procedure which includes predrying at elevated temperatures. This step leads to a greater amount of freezable water and thus to less freeze–thaw durability. It implies, as already noted, that the process alters the initial pores size distribution. In turn, this further implies that the predrying affects the absorption kinetics. Note also that the critical degree of saturation of 0.8 applies to the specific lower temperature noted above. Presumably, a lower degree of saturation would be needed for ice-immunity, albeit temporary, upon cycling to a lower temperature. Internal cracking still occurs for $S < S_c$, as evident from the reduction in the normalized modulus (Fig. 4), implying that even the drier material will eventually disintegrate.

Predrying at ambient temperatures appears to improve the durability during subsequent freeze–thaw cycles, at least of the type prescribed by ASTM C 666 (Thorpe 1996). An implication is that it may be difficult to correlate field performance, where predrying typically occurs before freezing, with performance in the laboratory where complete saturation usually precedes the cycle.

Aggregate

The aggregate is porous and thus vulnerable to ice damage. Porosities less than a few percent are generally desirable (Pigeon and Pleau 1995). Fine aggregate (i.e., <4.75 mm) is not an issue: this follows from the observation (MacInnis and Lau 1971) that the finest aggregates within material of various w/c ratios (0.6 to 0.45) led a stable product upon cooling to –18°C. On the other hand, in the same experiments coarse aggregate (10 and 20 mm) led to marked lengthening. This behavior is related more to the pore size distribution than to the total porosity, as evident form Kaneuji's (1980) tests [ASTM C 666(A)] on concretes made from 14 different types of aggregates. His results showed that the durability of the concrete increased with increasing coarseness of the aggregate pore system for a given aggregate pore volume (Fig. 5). The aggregate to avoid is the one with both a relatively high porosity (>5%) and a fine pore structure.

Type of cement

The type of cement appears not to be a major factor, at least in the freeze–thaw behavior of commonly used concretes where w/c > 0.45 (Tyler et al. 1951, Marchand et al. 1995) For drier concretes, however, the resistance appears to be better with finer cement (e.g., Type III vs. Type I). The im-
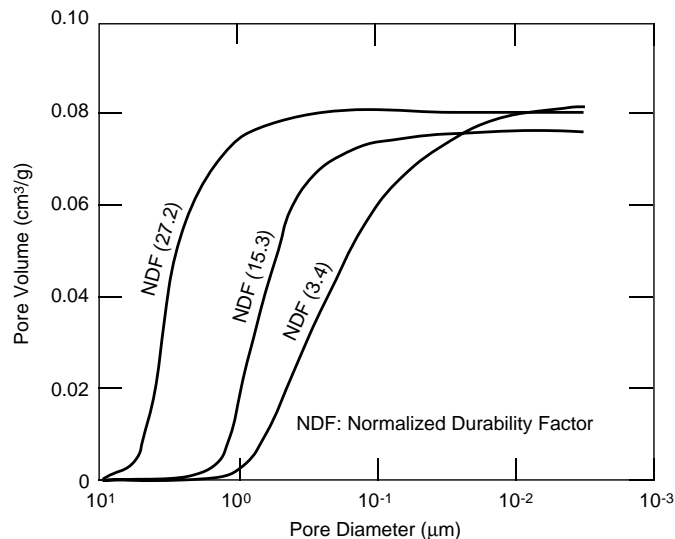

Figure 5. Showing the increase in resistance to ice damage with increase in average aggregate pore size (Kaneuji et al. 1980, from Marchand et al. 1995).

8

provement is manifested in terms of a larger critical air spacing factor (800 vs. 250 μm).

Freezing rate

The cooling/freezing rate is a factor in some situations. For example, Pigeon et al. (1985) found that when specimens (w/c = 0.5) of fully saturated material were exposed to 300 cycles of rapid freezing and thawing in air from 5° to –18°C and then assessed in terms of their increase in length, their resistance to ice damage (given in terms of the critical air-void spacing), albeit scattered, seemed to decrease with increasing freezing rate. Similarly, Nischer (1976) found that the salt-scaling rate of two concretes of different w/c ratios (0.45 and 0.70) exposed to 25 freeze–thaw cycles increased by about a factor of two upon increasing the freezing rate (to –20°C) by about a factor of two from 2.4 to 4.2°C/hr. On the other hand, salt-scaling tests (Sellevold 1988) showed a small but opposite effect, owing perhaps to the submerging of specimens in a salt solution.

More recently, Fagerlund (1992) has suggested that the freezing rate is probably not a factor when the material is sealed to prevent the exchange of moisture between the specimen and its surroundings.

Minimum temperature

Given that not all pore water freezes at the same temperature (more below), it would seem that the minimum temperature should be an important factor in ice damage. However, few data are available on this point. Marchand et al. (1995), in fact, suggest that the minimum temperature is not a factor. Pigeon and Pleau (1995), on the other hand, indicate that lower temperatures are more damaging. Perhaps it depends on how rapidly the material is cycled and, thus, on the time available for solidification. Kinetics, in other words, may be important.

Holding time

Similarly, few data are available on holding time. The indication, however, is that longer times are more damaging (Stark 1989). This factor may be important in the field where, relative to the laboratory, longer times and lower cooling rates are encountered.

Curing temperature

The curing temperature is a factor in high-performance material where the relatively low w/c ratio can lead to temperatures around 80°–90°C

during the early stages of hydration (Sellevold et al. 1994). Although few, the data indicate that the higher the temperature, the lower is the resistance to ice damage. For instance, during the cooling (at 3.3°C/hr) of water-saturated mortar (w/c = 0.50) to –11°C, about five times more ice formed (as detected calorimetrically) within material predried for three days at 50°C than within virgin mortar. Correspondingly, the predried and resaturated material lost through scaling about 18 kg/m^2 after 56 freeze–thaw cycles (SS 13 72 44), compared with about 1 kg/m^2 from the virgin mortar (Jacobsen and Selloveld 1993). Similarly, the average surface scaling of six different concretes (w/c = 0.45) cycled about 28 times in the presence of deicer salts (according to ASTM C 672) was 5 kg/m^2 after curing in moist heat at 65°C for 1 day compared with about 1 kg/m^2 after moist curing at normal temperature for 2 days. These effects have been attributed to a coarsening of the pore structure (Sellevold et al. 1994), despite the fact that mercury intrusion porisometry indicated that the pore size distribution shifted to smaller sizes upon warm curing.

That finer pores correlate with greater damage is consistent with the point noted about the vulnerability of aggregate. It is also consistent with the dictates of theoretical models discussed below (see *Thermodynamic Models*).

Silica fume

Silica fume (or microsilica) is a by-product of the production of ferrosilicon and is now commonly added to concrete to improve its strength (Roberts 1989). It occurs usually in the form of extremely fine, amorphous powder (0.1 μm) and typically constitutes about 5–10% by weight of the portland cement. It activates the pozzalanic reaction CH + S + H →C-S-H and effects a more uniform distribution of the hydration products. It also increases the length of the C-S-H polysilicate chain from around 2 to 4 units (Sellevold et al. 1994), as already noted.

Its effect on ice damage is inconsistent. For instance, the addition (10 wt. % of cement) to a normal concrete of w/c = 0.5 subjected to 300 rapid cycles of freezing and thawing in water (according to ASTM C 666A) reduced from about 500 μm to about 250 μm the critical spacing factor for entrained air bubbles. This implies a deleterious effect (Pigeon et al. 1986), and would be consistent with a refinement of the pore structure (Roberts 1989). In comparison, the addition (6 by wt. of cement) to concretes of lower w/c ratio (0.25–0.3)

made from Type-III cement (Pigeon et al. 1991) revealed little significant effect, as assessed through the same number/kind of rapid free-thaw cycles. On the other hand, silica fume (4–6%) added to roller compacted concrete of w/c = 0.4 reduced by about a factor of five the amount of spalling in the presence of deicing salts of specimens subjected to 56 cycles of the Boras test (Horrigmoe and Rindal 1990).

More systematic experiments are needed to fully assess whether, and if so under what conditions, silica fume affects ice damage.

Superplasticizers

Superplasticizers or water-reducing admixtures are generally added to concrete to increase either workability or strength or both. They are usually based on sulphonated melamine formaldehyde or sulphonated napthalene formaldehyde (Pigeon and Pleau 1995).

Their effect on ice damage appears to be rather small. For instance, Pigeon and Langlois (1991) showed through ASTM C 666 tests that the critical air spacing factor of two plain concretes of w/c = 0.5 with (10% by wt. cement) and without silica fume was not significantly affected by superplasticizers. And Thorpe et al. (1996) concluded from similar tests on 60 different mixes that superplasticizers do not negate the need for a well-developed system of air bubbles for freeze–thaw durability.

Alkalis

Alkalis are soluble impurities in cement. They stabilize the air-void system (Pigeon et al. 1992, Pistilli et al. 1983) and so might be expected to have a beneficial effect on the resistance to ice damage. On the other hand, should they assist cracking (see *Thermodynamic Models*) when concentrated at the ice/water interface, they could have a negative effect. Their role in ice damage is an open question.

Viscosity-modifying admixtures

Starches, gums, plant protein, and other natural polymers are sometimes added to thicken concrete mixes, to enhance cohesiveness and to lessen the separation of the constituents during transport, placement and consolidation (Izumi 1990). Concerning ice damage, welan gum and hydroxypropyl methylcellulose have little effect, at least on hardened concrete (w/c = 0.32, 0.40, and 0.45) when assessed using ASTM C 666 and ASTM C 672. Presumably, other additives of the same type

are equally benign. The only proviso is that an adequate (L_c = 250 μm) air-void system be maintained (Khayat 1995). If not, then the resistance is lowered (Fukudome et al. 1992).

Latex modification

Latex increases the fluidity of fresh concrete and significantly improves the resistance to both internal microcracking and surface scaling (Bishara 1979). Bordeleau et al. (1993) quantified the effect through experiments on limestone cements of three w/c ratios (0.30, 0.35, 0.40) containing zero, 7.5 and 15% (by weight of cement) styrene butadiene. The specimens were moist-cured for three days, and then subjected to 100 freeze–thaw cycles in the presence of a 2.5% NaCl solution, in accordance with ASTM C 672. In terms of the scale produced, the 100-cycle deterioration was around 1.6, 0.6, and 0.1 kg/m^2, respectively, for the 0, 7.5 and 15% additions.

Latex stabilizes air bubbles (Bordeleau et al. 1993) and refines the pore system. For instance, Ohama et al. (1985) found that the average pore radius (nm)/pore volume (cm^3/g) of a particular concrete decreased from about 100/1000 to 45/650 to 15/480 upon increasing the styrene butadiene concentration from 0 to 9 to 17% (by weight of cement). The latex may also coat the surface of the pores, thereby reducing the wetting angle. Which, if either, modification accounts for the effect is not known. However, for reasons which will become apparent (see *Thermodynamic Models*), pore refinement is not considered to be beneficial.

A latex-modified surface layer, although initially more expensive from the perspective of materials cost, would seem like a effective method for reducing ice damage to pavements and bridge decks and thus for increasing their service life.

Sealants

Sealants seem to impart little improvement. For example, Litvan (1992) examined eight types of mortar (cement: sand = 1 : 2) and 57 different organic and inorganic sealants. The specimens were contaminated with NaCl, dried, coated, and then subjected to 300 freeze–thaw cycles [ASTM C 666(A)]. Resistance to ice damage was assessed in terms of the residual expansion. Based upon 0.02% expansion, the sealants effected little consistent improvement. In fact, certain sealants actually lowered the resistance. Sedran et al. (1993) also found a deleterious effect, with oligomeric siloxane and polymeric siloxane: both sealants increased scaling in the presence of NaCl solution by a factor of

six. The reason for the negative results is not clear, but may be related to the possibility that sealants impede not only the entry of water, but also its expulsion.

Incidentally, Wyner (1995) recently patented a method for introducing into concrete pavement a polymeric resin, using a high pressure air gun, claiming protection against ice damage. Given the inconsistent results noted above, skepticism seems appropriate.

Microfibers

The possibility of suppressing ice damage through the incorporation of microfibers has not been examined (Pigeon and Pleau 1995). Perhaps it should be, given the beneficial effects of fibers on strengthening and toughening of concrete (Ouyang and Shah 1992, Banthia 1992, Tjiptobroto and Hansen 1993, Mindess 1994, Low et al. 1994). Fibers act as both load-carrying and crack-bridging elements. As such, they could increase the crack tolerance of the C-S-H matrix, provided that they are fine enough.

Possible candidates are steel and carbon, in recognition of current research on these materials in concrete (Mindess 1994, Ouyang and Shah 1992). A better fiber in terms of cost may be the naturally occurring mineral Wollastonite; i.e., calcium meta-silicate (β-CaO-SiO$_2$). This material has been used in the development of phosphate cement for dental applications (Bathnia and Sheng 1990) and in the production of tiles and cement boards (Semler 1975, Otouma et al. 1979). More recently, Low et al. (1992, 1993, 1994) established that these fibers (2–21% by volume; 25-diam. $\times$ 50–600 μm), roughly double the flexural strength and toughness of portland cement (w/c = 0.35). When combined with silica fume (about 10% by weight of cement), the Wollastonite more than tripled the values of these properties.

In pursuing further the possibility of fiber-enhanced durability, attention should be given to fiber length relative to crack size. For short cracks, long fibers impart greater strength but less toughness than short fibers (Budiansky and Cui 1995).

Applied load

Concrete in service is usually loaded, yet there is almost no literature on whether load affects the freeze–thaw resistance. The only published study appears to be one by Zhou et al. (1994). They applied static flexural loads of up to 50% of the failure load to both air-entrained and non-air-entrained beams of relatively dry mortar with (about

Table 2. Summary of the factors.

Intrinsic	Extrinsic
w/c ratio (M)*	Degree of saturation (M)
Entrained air (M)	Freezing rate
Aggregate	Minimum temperature
Type of cement	Holding time
Silica fume	Curing temperature
Superplasticizers	Sealants
Alkalis	Applied load
Viscosity— modifying admixtures	
Latex modification	
Microfibers	

*Major effect

10% by weight of cement) and without silica fume, and then measured the dynamic elastic modulus, after rapidly cycling the specimens according to a modified ASTM C 666 procedure. The load had no effect on the air-entrained material, but increased significantly the damage to the non-air-entrained mortar. For instance, a load of 50% of the failure load reduced by more than a factor of four the number of cycles required for disintegration. The effect on the non-air-entrained material was lessened through the addition of silica fume and was essentially eliminated by both adding silica and lowering the w/c ratio from 0.35 to 0.25. In wetter mortars (w/c = 0.45), however, silica fume was ineffective in suppressing damage to the non-air-entrained material. It thus seems that preloading is not a major issue, as long as air entrainment is incorporated. However, firm conclusions require further work.

Summary

Table 2 summarizes the ice damage factors. M implies a major effect.

ICE DAMAGE MECHANISMS

In considering the damage mechanisms, the problem is to understand the interaction between the pore water and the C-S-H matrix. "Bound water" (the interlayer water plus that adsorbed as a monolayer or so on the surface of the pores) is usually not considered because it does not begin to freeze until the temperature is lowered to –78°C (Powers and Brownyard 1947). A complete understanding of the problem probably requires the consideration of all water for, as we shall see, ice damage is related in part to the movement of water. In some cases, this movement may be facilitated by

the bound water. The movement of water, incidentally, is also fundamental to the creep of concrete (Hansen and Young 1991, Bazant 1972, 1982, 1995).

The destructive pore water C-S-H interaction results from the formation of ice, either internally, externally or both. Nucleation is usually not an issue. In principle it can be suppressed owing to supercooling (Helmuth 1960, Grubl and Stokin 1980)—in fact, has been suppressed to as low as –15°C (Helmuth 1960). In practice, however, nucleation occurs quite easily because there are usually enough sites at which heterogeneous nucleation can occur, such as the external surface or the surface of an entrained air void. The implication is that freezing begins somewhere in the system at a temperature close to 0°C, as observed (Powers and Helmuth 1953, Beddoe and Setzer 1988). The issue, therefore, is the growth of ice within the network of pores.

Early explanations invoked the "milk bottle" effect. The idea was that the interaction results simply from the 9% expansion in volume that accompanies the liquid-solid transformation. Perhaps something of this kind occurs at isolated sites where, as Bazant et al. (1988) suggest (after Powers et al. 1959), the pores may not be interconnected. However, following Powers (1945), better explanations recognize that concrete is not a closed vessel. The pore water within it not only freezes, but also migrates under the appropriate driving force, thereby creating in some way the internal disruptive tensile stresses that generate the damage.

The following discussion proceeds from the basis that the solidification and the movement of water are key to understanding damage. Essentially, two kinds of model are considered, one in which water migrates from the freezing sites, the other in which water migrates toward them.

Hydraulic pressure theory

The hydraulic pressure theory (Powers 1945, 1949) holds that the expulsion of water from the freezing sites creates stresses within the walls of the pores, much like water flowing through a hose creates hoop stresses. When sufficiently large, the stress ruptures the wall. The attractive feature of this model is that the maximum pressure P_{max} can be quantified in terms of the viscosity of the water η, the degree of saturation s, the rate of ice formation u, the rate of cooling c, the permeability κ, and the maximum distance the water must travel to the escape boundaries λ. Accordingly (Powers 1949),

$$P_{max} = \eta(1.09 - 1/s)\,uc\lambda/3\kappa. \qquad (1)$$

The model thus accounts for the effects of saturation and of entrained air (λ decreases as air porosity increases) and it recognizes the importance of capillary porosity through its direct relationship to permeability. Also, it accounts for expansion during freezing (Powers and Helmuth 1953). In predicting an effect of cooling rate, however, it contradicts the generally observed absence of such an effect (Fagerlund 1992). Also it fails to account for damage to/expansion of non-air-entrained cement paste under constant temperature (Powers and Helmuth 1953).

Thermodynamic models

The second kind of model is based upon equilibrium thermodynamics and considers the movement of water toward the freezing sites. An important concept is the chemical potential and its gradient, along which H_2O moves.

Chemical potential of a species is expressed in terms of molar free energy and activity. For a single-component system the activity is unity, and so the chemical potential and the molar free energy are the same. For equilibrium between ice and water, for instance, the chemical potential of H_2O must be the same in both phases. The chemical potential μ is a function of both temperature T and pressure P, and changes in potential may be expressed by

$$d\mu = VdP - SdT \qquad (2)$$

where V is the molar volume and S is the molar entropy. Vapor is more entropic than the condensed phases and water is more entropic than ice. A change in temperature, therefore, has the largest effect on the chemical potential of water vapor and the smallest effect on the potential of ice. Similarly, gases have the largest molar volume, and so a change in pressure has the largest effect on the chemical potential of the vapor. The molar volume of ice is greater than the molar volume of water, and so a change in pressure has a greater effect on the chemical potential of ice than water. Considerations like these account for the H_2O pressure-temperature diagram.

Freezing point depression

Now consider the water within the pores of cement, say at a temperature just above the normal freezing point of bulk water. It is held there by capillary forces and is assumed to be in equilib-
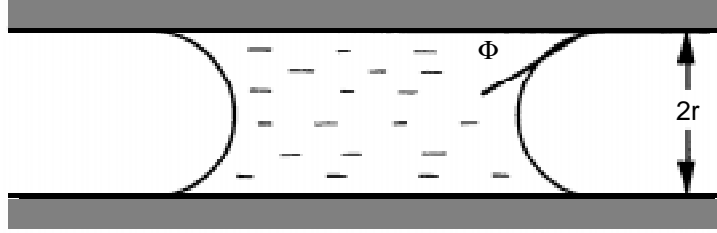
Figure 6. Schematic sketch of water within a capillary pore.

rium with the vapor. Wetting is defined by the angle Φ (Fig. 6), given by

$$\cos \Phi = (\gamma_{vw} - \gamma_{lw})/\gamma_{lv} \qquad (3)$$

where γ_{vw} = vapor/wall interfacial energy
γ_{lw} = liquid/wall interfacial energy
γ_{lv} = liquid/vapor interfacial energy.

Based upon adsorption/desorption and expansion/contraction studies (Amberg and McIntosh 1952, Feldman 1970), water is separated from the vapor by a meniscus concave toward the liquid. The meniscus creates negative pressure ΔP within the liquid; i.e., the water is under tension. For cy-lindrically shaped pores of radius r the pressure difference is given by

$$\Delta P = 2\gamma_{lv} \cos \Phi/r. \qquad (4)$$

In other words, the negative pressure lowers the chemical potential of water by the amount

$$\Delta\mu_l = V_l \Delta P \qquad (5)$$

where V_l is the molar volume of water (Fig. 7). The implication is that the freezing point of the capillary water is also reduced, by an amount given by (see App. D)
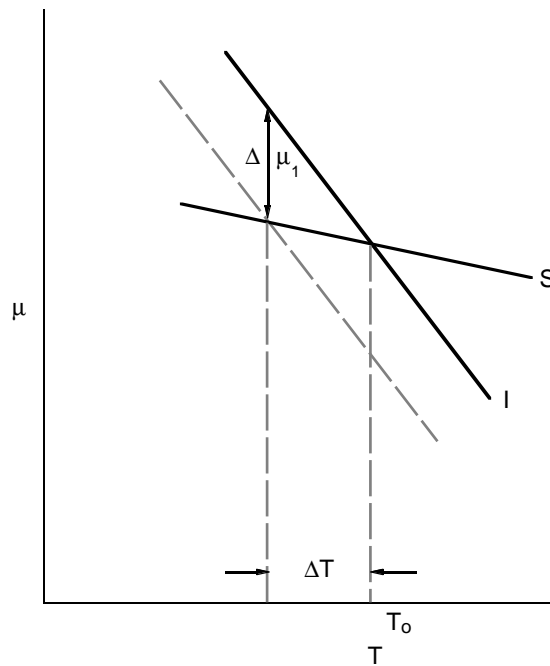
Figure 7. Schematic sketch of chemical potential of water (l) and ice (s) vs. temperature, showing the lowering of the freezing point by reducing the potential of water.

13

$$\Delta T = -2T_o\,\gamma_{lv}\,V_l\cos\Phi/Lr \qquad (6)$$

where T_o is the normal freezing point and L is the molar latent heat of fusion (taken here to be a positive quantity). The smaller the pore, the greater is the suppression. For instance, assuming complete wetting ($\Phi = 0$) and using $\gamma_{lv} = 75.7$ mJ/m^2 (the value at 0°C, Petrenko 1994), $V_l = 1.8 \times 10^{-5}$ m^3/ mole and $L = 6.04 \times 10^3$ J/mole, the freezing point of the water within pores of 100-, 10-, and 1-nm radius, respectively, is estimated to be –0.6°, –6.1°, and –55°C.

A distribution of pore sizes thus implies a range of freezing points. This point is in agreement with the emission of heat over a range of temperatures (Sellevold et al. 1994) during the cooling of fully saturated hardened cement. It is also consistent with results from quasi-elastic neutron scattering (El-Korchy et al. 1995), which show that hardened portland cement contains unfrozen water at sub-zero temperatures as low as –40°C.

Crystal pressure theory

Not clear from the above analysis is how the disruptive internal pressure develops, nor how saturated cement continues to expand at a constant temperature. These points can be understood by considering crystal growth (Everett 1961).

To begin, it is important to recognize that water is not the only liquid that can damage cement. For instance, benzene dilates saturated hardened cement paste (w/c = 0.5) when cooled at 2.5°C/s from room temperature to –20°C (Beaudoin and MacInnis 1974). The dilation begins at 5°C where the absorbate begins to freeze. Similarly, organic liquids induce expansion of porous Vycor glass upon cooling to below their bulk freezing points (Litvan 1972a, Kipkie et al. 1972), benzene expands saturated soil (Hoekstra et al. 1965), and organic liquids damage rock (Everett 1961). In each case the organic liquid *contracts* upon freezing. The damage to the host is caused by crystal growth.

To understand crystal growth and how it generates disruptive internal stresses, consider an Everett-type (1961) analysis. He modeled an idealized system that consisted of two large water-filled cylinders, each closed by a piston and joined by a narrow capillary tube, again in terms of equilibrium thermodynamics. We adopt the same approach, but imagine instead a series of water-filled globular-like large pores connected to each other and to the external surface (and to internal surfaces like air pockets) through a series of small capillary tubes. Two or more tubes of different radii connect at least some of the large pores. To estimate the response of the system upon cooling, we simplify the picture by considering a two-pore "unit element" (Fig. 8) analogous to Everett's cylinders.

As heat is extracted and the temperature falls, freezing is assumed to begin in one of the globular pores just below 0°C, say at a preferential nucleation site, such as a piece of dirt or an asperity on the wall. As the ice forms, it occupies a greater volume than the water consumed. This could create an excess pressure within the freezing pore should the rate of freezing be too fast to allow water to flow through the capillaries to the surfaces. Following Everett (1961), we assume that this buildup does not happen. Instead, we assume
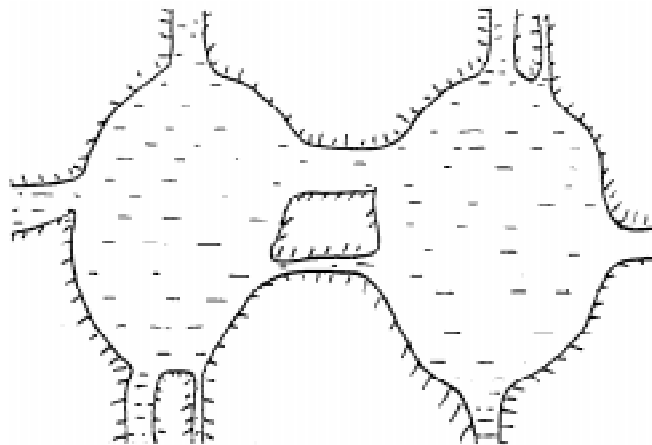

Figure 8. Sketch showing a saturated, multiply connected, two-pore element at a temperature above the freezing point of bulk water.
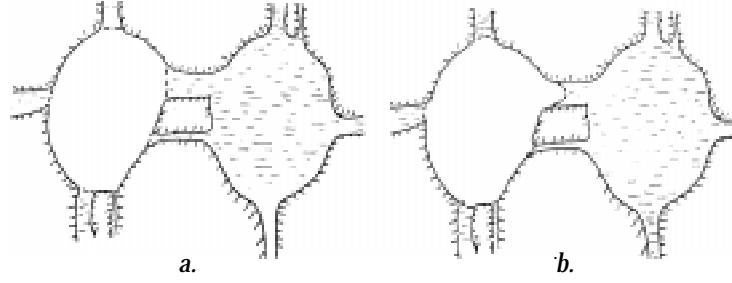
Figure 9. Sketch showing the solid/liquid interface (dotted) at two temperatures below the bulk freezing point T_z: a) at $T_p < T_l < T_o$ ice has filled the larger pore, but is confined to this pore; b) at $T_a = T_p$ ice bulges into the larger connecting capillary tube.

that freezing continues, but without building pressure until the crystal fills the pore. Freezing then continues in one of two ways. Either H_2O is drawn through the capillaries to the crystal from the water within the adjacent unfrozen pore through migration down a chemical potential gradient (the liquid has a higher potential than the solid), or the ice penetrates the mouth of the largest connecting capillary tube.

The first process leads to the ice expanding against the C-S-H walls and, in turn, to swelling of the cement. Initially, this process is the easier one. However, as the crystal grows against the constraint of the wall, say by the migration of H_2O through the unbound water layer, it becomes compressed and this raises its chemical potential, thereby lessening the gradient down which H_2O moves. At the same time, the ice in the mouths of the connecting capillary tubes begins to bulge out. Spherical bulge caps are assumed (Fig. 9) after Skapski et al. (1957) who observed such caps at the ice/water interface in fine glass capillary tubes. The radius of curvature of the cap is such that the attendant increase in the chemical potential of the ice within the bulge is equal to the increase in potential of the ice constrained by the wall of the large pore. The ice everywhere then has the same elevated chemical potential. For freezing to continue, more heat must be withdrawn and so the temperature must fall: otherwise, the ice begins to melt as its pressure increases. Eventually, however, as the crystal continues to grow by the migration of water down the chemical potential gradient, the pressure exerted against its constraint reaches the point that the radius of curvature of the ice within the bulge decreases to the radius of the largest capillary. At this point, the ice begins to penetrate the tube. Freezing then continues through the second process and the swelling stops.

The excess pressure ΔP_p at which ice crystal growth initiates penetration (provided that the wall has not ruptured by this time) is given by

$$\Delta P_p = 2\gamma_{sl}(1/r - 1/R) \tag{7}$$

where γ_{sl} is the ice/water interfacial energy (29.1 mJ/m^2, Hardy 1977), R is the radius of the large, globular pore, and r is the radius of the largest capillary. This is achieved at a temperature T_p given by (see App. D)

$$T_p = T_o(1 - V_s\Delta P_p/L) \tag{8}$$

where V_s is the molar volume of ice (2×10^{-5} m^3). For example, penetration into capillary pores of 100-, 10-, and 1-nm radius connected to much larger globular pores is expected to occur, respectively, at –0.5°, –5.3°, and –57°C; i.e., at a temperature similar to the expected freezing point of the capillary water. Correspondingly, the excess pressure ΔP_p is expected to be about 0.6, 6.0, and 60 MPa. Assuming that the pore wall is about as thick as it is wide, localized hoop-like tensile stresses of similar magnitudes are expected. Presumably, it is these stresses that ultimately induce the internal microcracking, if not during the first cycle then during subsequent cycles after the wall has been weakened through a kind of thermal fatigue.

This analysis thus accounts for the disruptive internal pressure underlying ice damage. The lower the temperature, the higher is the pressure and wall stress. Also, in invoking crystal growth through the transfer of H_2O down the chemical potential gradient, it accounts for the continued expansion of cement at a constant temperature. Moreover, it implies that such constant-temperature growth should stop once the chemical potential of the ice and water becomes equal, and that it

15

would resume once the temperature is lowered to a new level and held. The analysis also indicates that the factor that controls the pressure, and thus the wall stress, is the size of the *largest* capillary leading out of it (Everett 1961). This implies that the detailed fine capillary structure relative to the structure of the coarse pores is extraordinarily important to ice damage. Supporting the last point is Litvan's (1983) observation, already noted, that his more damage-resistant cement contained a greater volume fraction of intermediate sized pores. Also supporting it is Sellevold et al.'s (1994) correlation of greater resistance of deicer salts upon coarsening the pores. In other words, the analysis implies that the freeze–thaw durability of concrete increases as pore the structure coarsens.

That a coarser pore structure may impart greater freeze–thaw durability is not surprising. The realization is already incorporated in so-called durability functions (e.g., Bortz et al. 1990) for masonry. The problem is to quantify the microstructure (Livingston et al. 1995) and to know which measure to use in making predictions. The internal pressure develops in response to the increase in the ice/water interfacial area relative to the increase in the volume of the ice crystal (Everett 1961) *dA/dV*, but it is not clear how to measure this ratio.

How to coarsen the gel pores is a practical challenge. Some guidance/encouragement may be taken from Groves (1985). He noted from a transmission electron microscopy study of C-S-H that the gel pores in thin foils coarsened during observation. Either the heat of the electron beam was responsible or the electron irradiation was, or both. Particle irradiation would not be practical. Heating may be. Weakening through coarsening would probably not be a risk, because the strength-limiting flaws are orders of magnitude larger than the gel pores (Kendall et al. 1983).

Effect of air entrainment

Within the context of the crystal pressure theory, the beneficial effect of air entrainment can be explained in two ways. One explanation is essentially the one given by Powers and Helmuth (1953). Accordingly, the bubbles, should they contain water, act either as preferential or alternative sites for ice growth. They then compete for water with the ice within the large pore, for the chemical potential of the ice within the bubble would be lower, owing to the absence of a constraint to its growth. This has the effect of reducing the growth in the

large pore and, thus, of reducing swelling. How much the growth is biased in favor of the air bubbles depends upon the appropriate chemical potential gradients, and this depends upon the average spacing of the bubbles. The bias also depends on the transport mechanism, which may be different for the two sites (more below).

The other explanation is that the bubbles act as internal spaces of low relative humidity, which draw water from the connecting fine capillary tubes, thereby creating water/vapor menisci concaving toward the water. In so doing, a negative pressure develops within the liquid of each tube, of magnitude given by eq 4. This negative pressure reduces the excess pressure on the ice at the point of penetration, thus lessening the swelling. The ice is then both "pushed/extruded" and "pulled/drawn" through the capillary tube. Given that the growth along the tube increases the ice/wall interfacial area and decreases the water/wall area (and given that the former is more energetic than the latter, one could imagine a kind of "ice flow" resisted by surface drag or "friction," in which case the longer the tube the more resistive the "flow." The critical spacing factor L_c could then be viewed as the spacing below which the excess pressure never reaches the tensile strength of the C-S-H.

The latter view suggests a different interpretation of certain observations. For instance, perhaps the latex effect (see *Latex Modification*) is caused by a reduction in the "friction coefficient." Perhaps variations in the critical spacing factor from one concrete to another reflect variations in the appropriate interfacial energies through variations in the chemistry and structure of the capillary walls. Direct observations of the wetting angles in each of these cases, though difficult to make, would be informative.

Deicer salt degradation

Concerning the deleterious effect of deicer chemicals, two explanations come to mind. One follows directly from the crystal pressure theory and invokes the possibility of a kind of stress corrosion cracking. The chemicals/impurities and localized stress may act in a synergistic manner to crack the wall of the pore over time. Enhancing the action may be the concentration of the solutes at the ice/water interface; i.e., chemical concentration within a region where the stress is also concentrated. Speculative though it is, the suggestion is reminiscent of static fatigue, which is well known in concrete (Mindess and Young 1981), and

of subcritical crack growth (Bailey 1983).

The other explanation invokes a dendritic ice/water interface. Such interfaces recently have been observed (Montiero et al. 1995, Wang et al. 1996) during the freezing of 0.7 M alkaline solutions (Ca(OH)$_2$, KOH, NaOH). They are significant because, if characteristic of the interface within the highly alkaline cement pore water, they imply a greater increase in interfacial area per unit increase in volume of ice dA/dV than obtained for a spherical interface (for which $dA/dV = 8\pi r\,dr/4\pi r^2 dr = 2/r$ where r is the radius of the crystal). Correspondingly, the crystal pressure and wall stress will be greater. Dendritic interfaces develop owing to the buildup of impurities ahead of the interface and to the attendant lowering of the freezing point, which leads to constitutional supercooling, after Chalmers (1964) and coworkers.

These two explanations could be distinguished experimentally by measuring the internal stress. In the stress-corrosion cracking model, the chemicals do not increase the stress for a given subzero temperature, but just increase its action. In the dendritic interface model, the chemicals are expected to increase the pressure.

Internal stress

So far, nothing has been said about the internal stress, other than to indicate how it may develop and how to estimate its magnitude. Measurements are needed. Perhaps they could be made using neutron diffraction. The idea is to exploit the "internal" strain gauges represented by the crystal lattice of the crystalline CH phase or of any of the other single crystalline constituents of concrete. (Ice itself would probably not work because at the temperatures of interest stresses would relax relatively quickly.) Should the stresses/strains be large enough, they may distort/displace the diffraction pattern sufficiently to allow their measure. It may be useful to use heavy water to reduce the incoherent background (Steele and Sokol 1994).

Kinetics

Both the hydraulic theory and the crystal pressure theory can account for the internal pressure, which damages concrete upon freezing and thawing. The relative importance of each mechanism probably depends upon the cycle time. If cooling occurs very slowly, then there is little need to drive water quickly ahead of an advancing solid/liquid interface, and so the hydraulic pressure will be low. In this case, time is available for the system to approach equilibrium, if not to actually reach it. The thermodynamic approach would then seem to be the appropriate one. On the other hand, if freezing occurs quickly, then time is not available for equilibrium to be established. In this case, the hydraulic model is probably the more appropriate one.

How slow is slow enough for equilibrium to prevail is not clear. The kinetics depend upon the transport mechanism and on the transport distance, and these points have not been established. The general mechanism is almost certainly diffusion (Helmuth 1961), as evident from the dependence on time of dimensional changes in cement pastes (Powers and Helmuth 1953, Helmuth 1961)—mass diffusion and not thermal diffusion since thermal diffusivity is orders of magnitude larger than mass diffusivity. Surface diffusion along/within the thin layer of bound water on the pore wall is a specific candidate, but whether this dominates is unknown. Volume diffusion might also be important. Both mechanisms are thermally activated, presumably with different activation energies. This difference, however, is not easily exploited in a mechanistic search, because other factors that affect the mass transport rate, mainly the chemical potential gradient, are also thermally sensitive.

Assumptions

In presenting the above analyses not all of the assumptions were stated. Implicit are the following.

Thermodynamic properties of pore water: The analyses assumed that the thermodynamic properties of pore water are the same as those of bulk water. This is probably true for the largest pores, but not true for the smallest ones. In the latter cases, adsorbed water, and possibly layering and orienting of the surface molecules (Du et al. 1994, Porter and Zinn 1993) may affect the properties and thus the wetting angle, in ways not yet known. That thin layers of water do not possess the same thermodynamic properties as bulk water is evident from calorimetric and length measurements of porous Vycor glass, for instance, where around three monolayers of unfrozen water appear to remain at –40°C (Antoniou 1964). The difference is also evident from measurements of the dynamic elastic modulus of the same material, which indicate that only a fraction of the water is frozen at –40°C, the remainder transforming around –85°C (Sellevold and Radjy 1976).

How small is small probably depends on the

size of the H_2O molecule and on the number of molecules for bulk behavior. Kern and Karplus (1972) suggest that to a good approximation the molecule as water may be regarded as a sphere of radius 0.282 nm, which has embedded within it two positive and two negative charges, located at the vertices of a regular tetrahedron. This means that spherical pores of 1-, 10- and 100-nm diameter, for instance, contain about 5, 5000, and 5 million molecules. If bulk behavior requires about a million molecules, then a small pore would be less than about 50 nm in diameter. In other words, the thermodynamic properties of the water held within a large fraction of the gel pores may be different from the bulk properties.

Pore water composition: The analysis assumed that the pore water is a one-component system. In fact, OH^- and other ions are almost certainly present (Wang et al. 1996), particularly with deicer salts. While the ions probably have little effect in suppressing the bulk freezing point, they could lower the ice/water and ice/vapor interfacial energies, thereby lessening the freezing point depression. This would allow another explanation of the deleterious effect of deicer salts. The ions may also influence the transport kinetics should they concentrate at the pore wall where surface diffusion would operate.

Freezing sites: The analyses assumed that except near the free surface or near internal air voids, freezing takes place inside the material. Support for this view comes from several sources. Feldman (1970) studied length changes of porous Vycor glass at temperatures from –0.5 to –40°C upon adsorbing and desorbing water (vapor). The behavior was qualitatively similar to that above 0°C for the same material, which was well explained both qualitatively and quantitatively in terms of capillary condensation theory by Amberg and McIntosh (1952). The difference at subzero temperatures was a decrease in both the adsorptive capacity and the length change, features which Feldman attributed to the formation of solid (i.e., ice/water) menisci. Similarly, from volume expansion measurements, again upon cooling porous Vycor glass, Enustun et al. (1978) concluded that ice formed internally and not externally. Litvan (1972 a, b), on the other hand, concluded that water and ice never contact each other and that freezing occurs externally. Litvan's observations, however, were made with thin specimens and this probably affected the behavior.

The ice: It was assumed that ice I_h forms within the pores. While this is almost certainly true within the largest pores, where the water is expected to possess bulk thermodynamic properties, a different variant, possibly amorphous ice, might form within the smallest pores.

Thermal gradient: Isothermal conditions were assumed. In practice, thermal gradients are likely. This means that freezing probably begins near the outer surfaces. The basic mechanisms, however, are probably the same.

Air in bubbles: It was assumed that the air within the air bubbles plays no role. Enustun et al. (1994), on the other hand, suggested that its resistance to being compressed is a factor in the hydraulic pressure theory and that it biases the flow of water toward the free surface. This may trigger ice nucleation earlier than otherwise, but again probably does not affect the basic mechanisms.

RESEARCH NEEDS

Throughout this report questions have been raised, either explicitly or implicitly, about the structure of concrete and its behavior under cycles of freezing and thawing. These issues are summarized as follows and may be taken as (the author's view of) research needs:

Role of concrete microstructure in frost resistance

1. Is the outer product of cement hydration more vulnerable than the inner product to ice damage?

2. Is the tensile strength of C-S-H controlled by both the porosity of the outer product and the degree of polymerization (the length of the silicate chain)?

3. What are the true shapes, sizes and distributions of both the gel pores and the capillary pores?

4. What, if any, role does the interfacial transition zone play in ice damage to concrete?

5. What are the fundamental factors underlying the critical spacing of air bubbles and its effect in suppressing ice damage?

Analytical methods

6. To what extent can new methods of materials analysis, like neutron scattering and environmental scanning electron microscopy, help to improve our knowledge and understanding of ice damage?

7. Can the internal stress during freezing be measured from the lattice parameter of one of the crystalline phases, say CH?

Ice formation

8. Related to (5), is it the bubble spacing per se that is important, or is it a surfactant-induced reduction in one or more of the surface energies (ice/water, water/air, ice/C-S-H, water/C-S-H) that imparts resistance to ice damage?

9. Does ice damage increase as the minimum temperature decreases? As the holding time increases?

10. How different is the ice formation process in highly alkaline (pH = 12.5) solutions saturated in $Ca(OH)_2$ than in pure water, particularly within fine capillary and gel pores?

11. Is the exacerbation of ice damage by deicer salts caused by a kind of stress-corrosion-cracking? By the development of an unstable ice/water interface?

12. What form of ice, hexagonal cubic or amorphous, forms within the gel pores?

Improved frost resistance

13. Does ice damage decrease with increasing pore size?

14. Does silica fume affect ice damage? If so, how? If not, why not?

15. Will the incorporation of an appropriate distribution of fibers increase durability to freeze–thaw damage?

Modeling

16. The nucleation and growth of ice within the pores of concrete should be modeled. The model should be directed at the initiation, growth, and interaction of cracks. It should incorporate the pore water chemistry, the important aspects of the microstructure [pore size distribution, interfacial transition zone (?), entrained air], the degree of saturation, the appropriate thermodynamic properties (interfacial energies, enthalpy and entropy of both bulk and adsorbed water), and the important physical and mechanical properties (permeability, thermal expansion coefficients and conductivities, elastic moduli). The model should also include the fracture toughness of the cement and the complete thermal-mechanical history of the material.

LITERATURE CITED

Allan, A.J., R.C. Oberthur, D. Pearson, P. Schofield, and C.R. Wilding (1987) *Philosophical Magazine*, B, **56**(3): 263–288.

Amberg, C.H., and R. McIntosh (1952) *Canadian Journal of Chemistry*, **30**: 1013–1032.

Antoniou, A.A. (1964) *Journal of Physical Chemistry*, **68** (10): 2754–2764.

Ashby, M.D., and D.R.H. Jones (1986) International Series of Materials Science and Technology, Vol. 39, New York: Permagon Press.

Backstrom, J.E., R.W. Burrows, R.C. Mielenz, and V.E. Wolkodoff (1958) *Journal of the American Concrete Institute*, **55**: 261–272.

Bailey, J.E. (1983) Discussion *in Philosophical Transactions of the Royal Society of London*, A **310**: 124.

Bathnia, N., and J. Sheng (1990) *Proceedings, MRS*, **211**: 25–32.

Banthia, N. (1992) *Canadian Journal of Civil Engineering,* **19**: 26–38.

Barnes, B.D., S. Diamond, and W.L. Dolch (1978) *Cement and Concrete Research,* 8: 233–243.

Bazant, Z.P. (1972) *Cement and Concrete Research*, **2**: 1–16.

Bazant, Z.P. (1982) In *Creep and Shrinkage in Concrete Structuring* (Z.P. Bazant and F.H. Wittman, Eds.) London: John Wiley & Sons.

Bazant, Z.P., J.-C. Chern, A.M. Rosenberg, and J.M. Gaidis (1988) *Journal of the American Ceramic Society*, **71**(9): 776–783.

Bazant, Z.P. (1995) In *Materials Science of Concrete: IV* (J. Skalny and S. Mindess, Eds.), American Ceramic Society, p. 355–389.

Beaudoin, J.J., and C. MacInnis (1974) *Cement and Concrete Research*, **4**: 139–147.

Beddoe, R.E., and M.J. Setzer (1988) *Cement and Concrete Research*, **20** (2): 236–242.

Bergstrom, T.B., and H.M. Jennings (1992) *Journal of Materials Science*, **11**: 1620–1622.

Bishara, A.G. (1979) Federal Highway Administration, Report FHWA/OH/79/004.

Bordeleau, D., M. Pigeon, and N. Bonthia (1993) *ACI Materials Journal*, **89**: 547–553.

Bortz, S.A., S.L. Marusin, and C.B. Monk, Jr., In *Proceedings of the Fifth North American Masonry Conference (*D.P. Abrams, Ed.), The Masonry Society, Boulder, Colorado (1990), 1523–1535.

Budiansky, B., and Y.L. Cui (1995) *Mechanics of Materials*, **21**: 139–146. **Chalmers, B.** (1964) *Principles of Solidification*, New York: John Wiley.

Christensen, B.J., R.T. Coverdale, R.A. Olson, S.J. Ford, E.J. Garboczi, H.M. Jennings, and T.O. Mason (1994) *Journal of the American Ceramics Society,* **77** (11): 2789–804.

Darwin, D. (1995) In *Proceeding, MRS*, **370**: 419–428.

Du, Q., E. Freysz, and Y.R. Shen (1994) *Physical*

Review Letters, **72**, 238.

El-Korchy, T., D.L. Gress, R.A. Livingston, D.A. Neumann, and J.J. Rush (1995) In *Neutron Scattering in Materials Science* (D.A. Neumann, T.P. Russell, and B.J. Wuensch, Eds.), Pittsburgh: *Proceedings of the Material Research Society,* **376**.

Enustun, B.V., H.S. Senturk, and O. Yurdakul (1978) *Journal of Colloid and Interface Science,* **65** (3): 509–516.

Enustun, B.V., K.S. Soo and K.L. Bergeson (1994) *Journal of Materials in Civil Engineering,* **6** (2): 290–306.

Everett, D.H. (1961) *Transactions of the Faraday Society,* **57**: 1541–1551.

Fagerlund, G. (1971) *Materiaux et Constructions* (Paris), **4**: 271–285.

Fagerlund, G., (1973) *Materiaux et Constructions* (Paris), **6**: 215–225.

Fagerlund, G. (1977) *Materiaux et Constructions* (Paris), **10**: 217–230; bicl. 231–251.

Fagerlund, G. (1992) *Nordic Concrete Research,* **1**: 20–36.

Farran, J. (1956) *Review of Materials and Construction,* 490–4922.

Feldman, R.F. (1970) *Canadian Journal of Chemistry,* **48**: 287–297.

Feldman, R.F. (1981) *Proceedings of the Material Research Society,* p. 124.

FHWA (1995) Report to Congress: 1995 status of the Nation's surface transportation system. U.S. Federal Highway Administration.

Fukudome, K., K. Miyano, H. Taniguchi, and T. Kita (1992) *American Concrete Institute,* **SP-132**: 1565–1582.

Gagne, R., M. Pigeon, and P.C. Aïtcin (1990) *Materiaux et Constructions* (Paris), **23**: 103–109.

Gjorv, O.E., K. Okkenhaug, E. Bathen, and R. Husevag (1978) *Nordic Concrete Research,* **8**: 89–104.

Good, R.J. (1984) *Surface and Colloid Science,* **13**, 13.

Gregg, S.J., and K.S.W. Sing (1982) *Adsorption, Surface Area and Porosity.* London: Academic Press.

Groves, G.W. (1985) In *Microstructural Development During Hydration of Cement, Proceedings of an MRS Symposium,* vol. 85, p. 3–12.

Grubl, P. and A. Stokin (1980) *Concrete and Concrete Research,* **10**: 333–345.

Gu, P., and J.J. Beaudoin (1996) *Journal of Material Science Letters,* **14**: 1207–1209.

Hadley, D.N. (1972) Ph.D. Thesis, Purdue University.

Hall, C., W.D. Hoff, S.C. Taylor, M.A. Wilson, B.G. Yoon, H.W. Reinhardt, M. Sosoro, P. Meredith, and A.M. Donald (1995) *Journal of Material Science Letters,* **14**: 1178–1181.

Hansen, W., and J. Almudaiheem (1987) In *Proceedings of the Materials Research Society,* vol. 85, p. 105.

Hansen, W., and F. Young (1991) In *Materials Science of Concrete: II* (J. Skalny and S. Mindess), American Ceramics Society, Westerville, Ohio, 185–199.

Hardy, S.C. (1977) *Philosophical Magazine,* **35**: 471–484.

Helmuth, R.A. (1960) In *Proceedings of the 4th International Symposium on the Chemistry of Cement, Washington, D.C.,* VI-S2, 855–869.

Helmuth, R.A. (1961) *Proceedings, Highway Research Board Meeting,* **40**: 315–336.

Hirsch, T.J. (1962) *Journal of the American Ceramics Institute,* **59**: 427–452.

Hoekstra, P., E. Chamberlain, and A. Frate (1965) *Highway Research Record,* **101**, 30–32.

Horrigmoe, G., and D.B. Rindal (1990) Presented at 6th International Symposium on Concrete Roads, Madrid, Spain, 8-10 October 1990.

Izumi, T. (1990) *Concrete Engineering,* **28**.

Jacobsen, S., and E.J. Sellevold (1993) In *Proceedings from RILEM International Workshop on the Resistance of Concrete to Scaling due to Freezing in the Presence of Deicing Salts, August 30-31, Université Laval, Québec,* p. 231–246.

Jaegar, J.C., and N.G.W Cook (1979) *Fundamentals of Rock Mechanics.* 3rd ed., London: Chapman and Hall.

Jennings, H.M., and P.D. Tennis (1994) *Journal of the American Ceramics Society,* **77**(12), 3161–3172.

Justnes, H., I. Meland, I. Bjørgum and J. Crane (1990) *Advances in Cement Research,* **3**: 105–110.

Justnes, H., I. Meland, J.O. Bjørgum, and J. Krane (1992) *Proceedings of Application of NMR Spectroscopy to Cement Science,* Guerville, France, March 25-26.

Kaneuji, M., D.N. Winslow and W.L. Dolch (1980) *Concrete and Concrete Research,* **10**: 433–441 ASTM C 666A, p. 139.

Kendall, K., A.J. Howard and J.D. Birchall (1983) *Philosophical Transactions of the Royal Society of London,* A **310**: 139–153.

Kern, C.W., and M. Karplus (1972) In *Water—A Comprehensive Treatise* (F. Franks, Ed.) vol. 1, p. 21-91, New York: Plenum Press.

Khayat, K.H. (1995) *American Ceramics Institute Materials Journal.,* **92**(M64): 625–633.

Kipkie, W., R. McIntosh and B. Kelly (1972) *Journal of Colloid and Interface Science,* **38**: 3–11.

Kobayashi, M., K. Nakakuro, S. Kodama and S. Negami (1981) American Ceramics Institute Special Publication SP-68, American Concrete Insti-

tute, Detroit, p. 269–282.

Litvan, G.G. (1966) *Canadian Journal of Chemistry,* **44**: 2617–2622.

Litvan, G.G. (1972) *Journal of Colloid and Interface Science,* **38** (1): 75–83.

Litvan, G.G. (1972b) *Journal of the American Ceramics Institute,* **55** (1): 38–42.

Litvan, G.G. (1973) *Materiaux et Constructions (Paris),* **34**: 3–8.

Litvan, G.G. (1983) *Journal of the American Ceramics Institute.,* **80** (33): 326–331.

Litvan, G.G. (1992) *Concrete and Concrete Research,* **22**: 1141–1147.

Livingston, R.A., D.A. Neumann, A. Allen and J.J. Rush (1995) *Proceedings, Materials Research Society, Neutron Scattering in Materials Science* (D.A. Neumann, T.P. Russell and B.J. Wuensch, Eds.), vol. II, p. 376, 459–69.

Low, N.M.P., and J.J. Beaudoin (1992) *Concrete and Concrete Research,* **22**: 981–989.

Low, N.M.P., and J.J. Beaudoin (1993) *Concrete and Concrete Research,* **23**: 905–916.

Low, N.M.P., I. Gagnon, and J.J. Beaudoin (1994) *Advances in Cement and Concrete, Proceedings of an Engineering Foundation Conference, July 24-29, 1994, University of New Hampshire, Durham,* p. 200–216.

MacInnis, C., and J.J. Beaudoin (1968) *Journal of the American Concrete Institute,* **68** (3): 203–207.

MacInnis, C., and E.C. Lau (1971) *Journal of the American Concrete Institute,* **68**: 144–149.

Marchand, J., R. Pleau, and R. Gagné (1995) In *Materials Science of Concrete: IV,* edited by J. Skalny and S. Mindess, American Ceramics Society, Westerville, Ohio, 283–354.

Marsh, B.K., and R.L. Day (1985), *Materials Research Society, Proceedings,* Pittsburgh, **42**, 113.

Mather, B. (1978) In *Proc. of the First International Symposium on Superplasticizers in Concrete, Ottawa,* p. 325–345.

Mehta, P.K., and P.J.M. Montiero (1993*) Concrete Structure, Properties, and Materials.* 2d ed., Prentice Hall, Englewood Cliffs, New Jersey.

Meredith, P., and A.M. Donald (1995) *Journal of Materials Science,* **30**: 1921–1930.

Mielenz, R.C. (1968) In *Use of Surface Active Agents in Concrete, Fifth International Conference on Chemistry of Cement,* Tokyo, IV-1, p. 1–35.

Mindess, S., and J.F. Young (1981) *Concrete.* Englewood Cliffs, New Jersey Prentice-Hall, p. 171.

Mindess, S. (1994) *Advances in Cement and Concrete, Proceedings of an Engineering Foundation Conf., July 24-29, 1994, University of New Hampshire, Durham,* 217–222.

Monteiro, P.J.M., and P.K. Mehta (1985) *Concrete and Concrete Research,* **15**: 378–80.

Monteiro, P.J.M., M. Prezzi, K. Wang ,and V. Ghio (1995) Report No. UCB/SEMM-95/11, Department of Civil Engineering, University of California, Berkeley, 274pp.

Nischer, P. (1976) *Zement and Betond,* heft 2.

Ohama, Y. K. Notoya, and M. Miyake (1985) *Transactions of Japanese Concrete Institute,* **7**: 165–172.

Okada, E., M. Hisaka, Y. Kazama, and K. Hatori (1981) ACI-SP 68, 215-231.

Ollivier, J.P., and J. Grandet (1980) *Proc. of the 7th Inter. Cong. on the Chem. of Cement, Paris.*

Otouma, T., H. Asaumi, K. Kubota, and M. Yamamoto (1979) Use of Fibrous Wollastonite for Reinforcing, U.S. Patent no. 4,144,121, March 13.

Ouyang, C.D., and S.P. Shah (1992) *Cement and Concrete Research,* **22**: 1201–1215.

Parrott, L.J. (1986) in *Research on the Manufacture and Use of Cements,* Engineering Foundation, New York, p. 32.

Parrott, L.J. (1989) In *Materials Science of Concrete: I* (Jan P. Skalny, Ed.), The American Ceramic Society, Inc., Westerville, Ohio, p. 181–195.

Petrenko, V.F. (1994) U.S. Army Cold Regions Research and Engineering Laboratory Special Report 94-22, Hanover, New Hampshire.

Pigeon, M., R. Pleau and J.M. Simard (1985) *Journal of the American Concrete Institute,* **82** (5): 684–692.

Pigeon M., R. Pleau and P.C. Aïtcin (1986) *Concrete, Concrete and Aggregates,* 8(2): 76–85.

Pigeon, M. (1989) *Materiaux et Constructions* (Paris), **22** (127): 3–14.

Pigeon, M and M. Langlois (1991) *Canadian Journal of Civil Engineering,* **18**(4): 581–589.

Pigeon, M., R. Gagné, P.C. Aïtcin and N. Banthia (1992) *Concrete and Concrete Research,* **21**: 844–852.

Pigeon, M., P. Plante, R. Pleau and N. Banthia (1992) *ACI Mat. J.,* **89**: 24–31.

Pigeon, M. and R. Pleau (1995) *Durability of Concrete in Cold Climates.* London: Chapman and Hall.

Pistilli M.F. (1983) *ACI Journal, Proceedings,* **80**(3): 217–222.

Pope, A.W. and H.M. Jennings (1992), *Journal of Material Science,* **27**: 6452–6462.

Porter, J.D., and A.S. Zinn (1993), *Journal of Physical Chemistry,* **97**: 1190.

Powers, T.C. (1945), *J. Amer. Conc. Inst.,* **41** (4): 245–272.

Powers, T.C. (1949) *Proceedings, Highway Research Board Annual Meeting,* National Academy of Sciences, **29**: 184–211.

Powers, T.C. (1954) *Journal of the American Concrete Institute*, **50**: 741–760.

Powers, T.C. (1955) In *Proceedings of the American Society for Testing and Materials,* Vol. 55, ASTM, Philadelphia.

Powers, T.C. (1975) *ACI-SP-47-1,* American Concrete Institute, Detroit, 1-11.

Powers, T.C., and T.L. Brownyard (1946), *Journal of the American Concrete Institute,* **18** (8): 934–69.

Powers, T.C., and T.L. Brownyard (1947), *Journal of the American Concrete Institute*, **43**: 101, 993.

Powers, T.C., and R.A. Helmuth (1953*) Proceedings, Highway Research Board Annual Meeting,* National Academy of Science, p. 285–297.

Powers, T.C., L.E. Copeland, J.C. Hayes and H.M. Mann (1954) *Journal of the American Concrete Institute,* **26**(3), 51-14, 285–298.

Powers, T.C., L.E. Copeland, and H.M. Mann (1959) *Journal of the Portland Cement Association Research and Development Lab*oratory, **1**(2): 38–48.

Prasad, M., M. Manghnani, and R.A.Livingston (1996) *Proc. Japan.-U.S. Conf. on Non-Destructive Testing* (in press)

Rarick, R.L., J.I. Bhatty, and H.M. Jennings (1995) In *Materials Science of Concrete: IV* (J. Skalny and S. Mindess, EdS.), American Ceramics Society, Westerville, Ohio, 1-39.

Richardson, I.G., and G.W. Groves (1993) *Journal of Material Science,* **28**: 265.

Rindal, D.B., and D.B. Horrigmoe (1993) In *Third Inter. Symposium on Utilization of High-Strength Concrete, Lillehammer, Norway, 20–24 June 1993.*

Roberts, L.R. (1989) In *Materials Science of Concrete: I* (J. Skalny, Ed.), Westerville, Ohio: American Ceramics Society, p. 197–222.

Schaefer, D.W. (1994) *Materials Research Society Bulletin,* **19**: 14–17.

Scrivener, K.L., and E.M. Gartner (1988) *Proceedings of the Materials Research Society, Bonding in Cementious Composites*, p. 77-86.

Sedran, T., Pigeon M., and Hazroti K. (1993) In *Durability of Building Materials and Components,* S. Nagataki, T. Nireki and F. Torosawa, Ed., E.&F.N. Spon, London, p. 487–496.

Sellevold, E.J. (1988) SINTEF Report ST 65-A88090 Tech. Univ. of Trondheim.

Sellevold, E.J., and F. Radjy (1976) *Journal of Material Science,* **11**: 1927–1938.

Sellevold, E.J., and T. Farstad (1991) *Nordic Concrete Research,* **10**: 121–138.

Sellevold, E.M., H. Justnes, S. Smeplass, and E.A.

Hansen (1994) In *Advances in Cement and Concrete, Proceedings of an Engineering Foundation Conference, July 24-29, 1994, University of New Hampshire, Durham,* p. 562–609.

Semler, C.E. (1975) A quick-setting Wollastonite phosphate cement. Presented at the 77th Annual Meeting of the American Ceramics Society, Washington, D.C., May 6, (no. 5-jiii-75).

Sing, K.S.W., D.H. Everett, R.A.W. Haul, L. Moscou, R.A. Pierotti, J. Rouqueron, and T. Siemieniewska (1985) *Pure and Applied Chemistry,* **57**: 603.

Skapski, A., R. Billups, and A. Rooney (1957) *Journal of Chemistry and Physics,* **26**: 1350–1351.

Smith, D.M., D.W. Hua, and W.L. Earl (1994) *Materials Research Society Bulletin,* **44.**

Stark, D. (1989) *Portland Cement Association Research and Development Bulletin,* RD096, p. 191.

Steele, L.M., and P.E. Sokol (1994) *Bull. Amer. Phys. Soc.,* **39**: 359.

Tan, D.M. (1995) *Acta Metallurgical et Materialia,* **43**: 3701–3707.

Tarrida, M., M. Madon, B. Le Rolland, and P. Colombet (1995) *Advanced Cement Based Materials,* **2**: 15–20.

Taylor, H.F.W. (1986) *Journal of the American Concrete Society,* **69** (6): 464–467.

Taylor, H.F.W. (1992) *Cement Chemistry.* San Diego: Academic Press.

Thorpe, J.D. (see NCHRP February 1996) *Research Results Digest,* no. 208. 1–10.

Tjiptobroto, P., and W. Hansen (1993) *ACI Materials Journal,* **90**: 16–25.

Tyler I.Z., G.J. Verbeik, and T.C. Powers (1951) Report of the Portland Cement Association.

Vanderhorst, N.M., and D.J. Janssen (1990) In *The Freezing-and-Thawing Environment: What is Severe?, Paul Klieger Symposium on Performance of Concrete* (D. Whiting, Ed.), ACI Special Publication SP-122, Detroit, Michigan: American Concrete Institute, p. 181–200.

Verbeck, G.J., and R. Landgren (1960) *Proceedings, ASTM,* **60**: 1063–1079.

Viehland, D., J.F. Li,L.J. Yuan, and Z .Xu (1996) *Journal of the American Ceramics Society,***79**: 1731–1744.

Wang, K., P.J.M. Monteiro, B. Rubinsky, and A.Arav (1996) *ACI Materials Journal,* **96**: 370–377

Wyner, J.S. (1995) U.S. Patent No. 5,413,808, May 9.

Zhou, Y., M.C. Cohen and W.L. Dolch (1994) *ACI Materials Journal,* **91**: 595–601.

APPENDIX A: METHODS OF MICROSTRUCTURAL ANALYSIS*

This section considers the techniques that have been used to examine the microstructure of concrete. Appendices B and C list further details, and note the underlying principles, resolution, advantages, and disadvantages plus applications of both imaging and indirect techniques.

MICROSTRUCTURAL ARTIFACTS

A problem common with many of the techniques used to examine the microstructure of concrete is that they can affect the structure. Even if the technique itself is noninvasive, specimen preparation can affect the structure. For example, many techniques require that the specimen be prepared by mechanically polishing to produce either a flat surface or a thin specimen. This is particularly problematic for concrete because the different phases polish at different rates and pullout can occur. And, as with any material, surface damage can also occur during mechanical polishing. Another common problem is the need to dry the specimen before examination. This can severely affect the pore structure and may lead to chemical changes. Similarly, putting a concrete or cement specimen into a vacuum, which is necessary on some analytical instruments, will lead, unless the specimen is very old, to a loss of water and a change of structure. In this regard, concrete and cement, because of their high water contents, can almost be viewed in the same light as biological materials rather than as a typical ceramic material. Even examination in air, which at first sight may seem benign, can be a problem: carbonation of the cement surface can occur, which can particularly be a problem when using a type of radiation probe that is not very penetrating. Thus, whatever technique is used, it should always be borne in mind that the microstructure could be altered by either the technique itself or by specimen preparation. Thus, it is important that the microstructure be examined using more than one technique.

IMAGING TECHNIQUES

Imaging techniques can directly provide information on the amounts, sizes, shapes, and distributions of phases (or pores) within their resolution range, and in combination with other techniques may be able to both quantify the chemistry and identify the (crystal) structure.

The highest resolution of the instruments that have been applied to concrete/cement is a (scanning) transmission electron microscope, (S)TEM. In one of these instruments, the change from imaging to diffraction is at the push of a button. In combination with energy dispersive spectroscopy (EDS) electron energy loss spectroscopy (EELS), this type of instrument is sometimes referred to as an analytical electron microscope (AEM). An AEM is an extremely powerful tool and probably occupies the position as the pre-eminent analytical tool in materials science. In principle, it can be used to determine all of the microstructural/microchemical parameters of a material (on a scale small). Unfortunately, this technique is fraught with difficulties in its application to cement/concrete, the principal ones being the need for a high vacuum ($\leq 10^{-4}$ Pa) and the possibility of specimen damage under the high energy electron beam. The former problem has been mitigated to some extent by using environmental cells or differential apertures in the microscope which al-

---

*Prepared by I. Baker, Thayer School of Engineering, Dartmouth College.

23

low the specimen to be maintained in up to 4 kPa (300 torr) of water vapor. The latter problem can be mitigated in modern AEMs by the use of rapid beam-shifting programs that allow only the area of interest to be exposed to the electron beam during image collection.

The microchemistry of various phases in cement can be determined using EDS and atomic number contrast maps can be produce (Richardson and Groves 1993). However, this technique is usable only for elements of atomic number greater than five and is really best suited for higher atomic number elements (lighter elements tend to produce more Auger electrons than fluorescent x-rays under electron beam irradiation). Surprisingly, EELS does not appear to have been used on cement/concrete, even though it works best for detecting lighter elements. However, data are difficult to quantify. For microchemical analysis, both EDS and EELS require that a stationary probe be placed on the specimen for, say, 50–100 s. This can cause severe specimen damage.

Specimen preparation is also problematic for the TEM/STEM. The usual preparation technique for nonconductors, such as cement, ion-beam thinning, is notorious for causing specimen damage and in some materials, e.g., SiC, can even cause a phase transformation.

Even if the TEM/STEM were not fraught with problems, it cannot provide the big picture, but provides great detail of a small volume of material. This is particularly a concern in a material as heterogeneous as concrete. A scanning electron microscope, SEM, has often been used to examine cement/concrete. This instrument is extremely useful for examining fracture surfaces, because of the large depth-of-field possible, and can be used to obtain atomic number contrast from flat polished surfaces if backscattered electrons are used (secondary electrons give little contrast from such surfaces unless etched). The problems associated with the nonconducting nature of the cement and the rapid drying in the vacuum inside the microscope have been largely overcome in the last few years by the advent of the environmental scanning electron microscope, ESEM. Recent ESEMs are easy to use and can operate with up to ~270 Pa of water vapor in the specimen chamber. The ESEM's resolution is only marginally lower than that of a conventional SEM.

EDS can also be used in the SEM/ESEM to determine local chemistries and to produce atomic number contrast maps. An EDS system on a SEM provides a powerful tool for studying the microstructure of concrete, and the effects of the environment (corrosion) and freeze–thaw effects in situ. Wavelength dispersive spectroscopy (WDS) does not appear to have been used to examine concrete/cement. It has the advantage, over EDS, that lower atomic number elements can be detected ($Z \geq 3$) and the detection limits are lower; quantification can also be more accurate if several spectrometers are used simultaneously.

Diffraction information is also obtainable in a SEM. Recently, the electron backscattered pattern (EBSP) has been supplanting the selected area channeling pattern (SACP) technique as the way to obtain both crystal structure and orientation information in the SEM, since specimen preparation is less critical and information is readily obtainable from areas as small as 1 μm^2.

Scanning acoustic microscopy, which images differences in acoustic impedance, can provide a resolution up to 1 μm (1 GHz) and image up to about ~10 mm below the surface (100 MHz), allowing serial imaging, although not simultaneously. The technique has the advantage that concrete can be examined in the wet condition (water is used as the coupling medium between the lens and the specimen). However, it appears to have few advantages when compared to the ESEM for phase identification, size and distribution determination, since the resolution is much lower and the crystallographic (diffraction) and analytical capabilities available on the ESEM are not possible. The only advantage appears to be the capability of serial imaging down to about 10 mm without physically dissecting the specimen, although

only at a resolution of ~15 μm. The related techniques of scanning electron acoustic microscopy and scanning laser acoustic microscopy appear to have little advantage for the study of cement, since they do not utilize water as the coupling medium. Scanning acoustic microscopy is useful for imaging cracks by observation of the fringes produced by Rayleigh waves, and subsurface cracks less than 100 nm can be observed. Cracks have also been studied in using a number of standard "imaging" techniques: laser holographic interferometry, Moiré interferometry and photoelasticity. All have some difficulties (see App. B).

The related techniques of scanning or atomic force microscopy (referred to as either SFM or AFM), scanning capacitance microscopy (SCM), and scanning tunneling microscopy (STM), although having excellent (atomic level vertical) resolution, and also in the STM the capability of atomic number contrast on an atomic level, appear not to have been applied to cement or concrete. However, they are probably not very useful since they require the preparation of the surface on an extremely fine scale: for atomic level resolution, the SFM needs an atomically flat surface. STM also is probably unusable since specimens have to be conductors or semiconductors.

Optical microscopy is a standard technique for examination of cement and concrete with a resolution of 1 μm. Etchants can be used to study quantitatively the distribution of anhydrous phases in clinker and cement powder. In thin sections of hydrated pastes and concrete, the refractive properties of the different phases and the use of fluorescent resin can indicate the cement and aggregate type, the water/cement ratio, the presence of mineral admixtures, the quality of compaction, and the presence of alkali silica reactions. A recent variant (laser scanning) confocal optical microscopy could be used to study concrete/cement in the wet condition, although this does not appear to have been tried yet.

NONIMAGING TECHNIQUES

Nonimaging techniques cannot by themselves provide a complete description of the microstructure. In fact, a nonimaging technique requires either a (mathematical) model to relate whatever parameter is being measured to the microstructural feature of interest, or a standard to which measurements can be related. In some cases, the accuracy of the model limits the ability to describe the microstructure rather than a fundamental limit in the resolution or accuracy of the technique itself.

Bulk phase identification is routinely performed by x-ray diffraction (XRD), a standard materials technique. X-rays provide average data, rather than specific local information. The orientation of phases (texture) can also be determined on a scale as large as the incident beam (~1 cm^2). Although a conventional x-ray set can be used to follow phase formation during the hydration of cement, the time steps have to be quite large (~1 hr). The use of synchrotron radiation for this purpose would allow time steps of a few seconds to be used. This appears not to have been done, thus far. Neutron diffraction is similar to x-ray diffraction but has the advantage that neutrons are scattered much more strongly from some light atoms, e.g., H, than x-rays. Also, since neutrons are much more penetrating than x-rays thicker specimens can be used. The main problem is that access to a high intensity neutron source is necessary.

Raman spectroscopy can also be used to provide average information not only on the phases present, but also on the local bonding. The technique has the advantage over the conventional x-ray technique that the time resolution is typically 1 min. Thus, hydration can be followed over small time steps. However, the quantification of the phases present is worse than using x-rays. Nuclear magnetic resonance (NMR) can also be used to study the different local environment of water

molecules and, thus, can be used to follow hydration. Similarly, quasi-elastic neutron scattering probes the major dynamic modes of motion that characterize the state of the water molecule. The technique can be used to follow nondestructively the hydration of cement and to determine the distribution of water among various states, i.e., free, chemically bound or physically trapped and to investigate the formation of ice in pores. It has the disadvantage that it requires access to a high intensity neutron source. Even so, currently, it takes 1–2 hours to acquire a single datum point, thus seriously limiting the time resolution. The technique does not distinguish between adsorbed water and water trapped in gel pores, or between free water in capillary pores and larger pores. There are a number of specimen preparation problems with this technique (see discussion of SANS below).

An advanced form of impedance measurement, impedance spectroscopy, can be used to follow microstructural evolution over small (< 1 min) time steps noninvasively. Also, it provides a rapid method of determining the water/cement ratio. However, it is difficult to interpret results in terms of microstructural changes, and difficult to differentiate the contributions of the various factors that affect conduction, i.e., ion concentration, water content and pore structure. Most importantly, the accuracy of this technique depends on the model used to relate the microstructure to the electrical impedance.

For local chemical information from surfaces, x-ray photoelectron spectrometry (XPS), Auger electron spectroscopy (AES) or secondary ion mass spectroscopy (SIMS) can be used. Thus far, AES appears not to have been used on cement/concrete. All of these techniques provide information from material within only ~1 nm of the surface, and unfortunately all require the use of an ultra-high vacuum (UHV), which leads to rapid drying of the specimen if it is not already dried. Specimen imaging is possible at the same time in both AES and SIMS, using secondary electrons. Sputter depth profiling is possible with all these techniques, but has the problem that not all atomic species are sputtered at the same rate. In contrast to the other two techniques, XPS can give detailed information on the bonding or local environment. However, SIMS has the advantage that hydrogen is detectable, whereas it is not using the other two techniques.

Rutherford backscattering spectrometry (RBS) provides information on the local chemistry at a depth (< 10 μm) between that of x-rays and the above-mentioned techniques. Again, as with the above three surface techniques, it has the disadvantage that it must be performed in vacuum and has the additional disadvantage that only elements for $Z > 4$ are detectable. Thus far, this technique appears not to have been applied to the study of cement or concrete, and there appears to be little advantage in doing so.

The nanoindenter can provide information on mechanical properties on a very fine scale. The technique does not appear to have been applied to cement/concrete, but could provide information on a scale to which the surface can be mechanically polished, say 1 μm, allowing information to be obtained from individual phases in situ.

PORE EXAMINATION

Within porous materials in general pore sizes range over six to seven orders of magnitude (Smith et al. 1994), from fractions of a nanometer to several hundred microns. Thus, to examine pores, no single technique is entirely satisfactory and the values for the pore parameters can vary depending on the techniques used to measure them. For example, nitrogen absorption can measure pore sizes in the range 0.35 nm to 70 nm, whereas mercury intrusion porosimetry (MIP) is usable for pore sizes 3.5 nm to 200 nm. A problem with many techniques described in this

section, when applied to cement, is that the cement has to be dried, typically through heating, and this can change the pore structure, as already noted. However, solvent replacement, using methanol to replace the water, appears to preserve the original pore structure. Using this technique, the pore volumes obtained by a combination of nitrogen absorption (up to 4 nm), and MIP (for larger pores) produced excellent agreement between measured and calculated densities of cement (Hansen and Almudaiheem 1987).

There are numerous techniques for examining pores, as already noted. Perhaps, the most obvious techniques for the examination of both pore size and pore distribution are optical microscopy and scanning electron microscopy. However, these techniques are limited both by resolution (1 μm for optical microscopy; 0.1 μm for backscattered electrons on a scanning electron microscope) and by polishing that may damage or plug pores on the examined surface.

Ignition is a standard technique used to determine the evaporable water and, hence, the porosity. The technique assumes that all the evaporable water is removed before ignition. Permeability can be used to determine the porosity. Both total porosity and its distribution determine the permeability, but only pores greater than a specific value contribute to the permeability. The most common technique is measurement of the amount of water that can be forced into the specimen under pressure. There are a number of problems with this techniques. For example, for impermeable specimens, small specimens have to be used, which can lead to problems with lack of representativeness. Since the solubilities of phases vary with local hydrostatic pressure, pressure gradients through the specimen can lead to phase redistribution, which affects the pore structure and permeability. Permeability methods tend to give lower surface areas than absorption methods, see below, because of blocked channels that are not accessible to moving air/fluid streams.

There are a number of "standard" techniques for determining the pore size distribution and, even though they have often been used, many have problems. MIP was for many years the primary method for investigating pore-size distribution (total porosity, capillary porosity, and gel porosity) of hardened cement paste although it provides no information on the spatial distribution of the pores. As noted earlier, it is best used for pores in the range 3.5 nm to 200 μm (it is unusable for pore diameters < 2 nm), and provides the same results as helium pyncometry for plain dried pastes but in blended pastes MIP gives higher porosities (Marsh and Day 1985). There are a number of other problems with the technique, in addition to those noted above, including specimen damage from both the predrying and the high pressures involved; uncertainty in the contact angle and surface tension; and the network/percolation "ink-bottle" effects. The microstructure can be altered during mercury intrusion.

Another standard technique is gas (typically, nitrogen) adsorption. It can be used to measure both external surface area and is well established for mesoporous solids with pore diameters in the range 2–50 nm (for microporous solids where the pore diameter is less than 2 nm there is some uncertainty in interpreting data). As for MIP, no information on the spatial distribution of the pores is obtained and the structure can, again, be altered during (gas) intrusion. Finally, it is worth noting that the internal areas determined by gas adsorption are dominated by gel porosity, which has only a minor effect on bulk transport. Two related techniques are methanol adsorption and water adsorption. Both have similar problems to nitrogen adsorption and may give different values for the pore size distribution due to the differences in the polarity and size of the molecules. Again a fundamental flaw with the techniques is that large pores with small openings will be intruded at pressures corresponding to the entrance of the pore, resulting in a skewing of pore sizes.

The related techniques of small angle neutron scattering (SANS) and small angle

x-ray scattering (SAXS) are both useful for characterizing the gel pore surface and fractal dimensions. They have the advantage, compared to many of the above techniques, that they do not require drying of the specimen and are noninvasive, allowing the same specimen to be examined many times. SANS is probably the more useful of the two techniques since neutron absorption is much less than x-ray absorption, allowing the use of thicker specimens. Even so, specimens must be less than 1 mm thick to avoid multiple scattering. Again, such specimens are difficult to prepare from concrete. Also, carbonation of the surface can occur if care is not taken. Probably the main disadvantage with these techniques is that they are not easily accessible, requiring specialized x-ray or neutron sources.

NMR has also been applied to the determination of pore size distribution in some materials. However, it is not clear that appropriate mathematical models have been developed sufficiently in order to relate the measurements to pore sizes.

Two novel techniques for examining pore size distributions are low-temperature calorimetry (calorimetry is a standard technique for determining the course of hydration of cement via the heat output) and elastic modulus measurements. Using low temperature calorimetry, the heat change (which indicates the amount of water) and the temperature at which the change occurs (which indicates the water-filled pore diameter—the smaller the pore the lower the freezing temperature) can be measured during cooling. The technique avoids specimen predrying and can be used several times on the same specimen. It is best for larger pores. The elastic modulus method also requires cooling the cement/concrete specimen. By using mathematical models, knowing the elastic modulus of the components of the cement and determining the elastic modulus at a given temperature, the volume fractions of the components (ice/water) can be determined. Again the technique uses the fact that water freezes in small pores at a lower temperature than in large pores. Thus, to determine the pore size distribution, the elastic modulus is determined at different temperatures. In addition, ice damage can also be followed directly. There are two disadvantages with this technique: dynamic elastic modulus measurements are performed in vacuum, leading to water sublimation, and the validity of the results depends on the accuracy of the mathematical models.

APPENDIX B: IMAGING TECHNIQUES

Technique	Resolution	Advantages	Disadvantages
Transmission electron microscopy (TEM)	• Diffraction image –1 nm weak-beam –10 nm bright field •Lattice image –0.1 nm	Specimen is imaged in either transmission of forward-diffracted dark-field from a flood electron beam incident on the specimen. Has the advantage that both imaging, diffraction and other microchemical analytical techniques can be used simultaneously (see below). In principle, even the finest features of the structure can be imaged and identified. There have been several studies of dried ion-beam thinned specimens of both cement and concrete[1]. Cement pastes can be examined wet in an environmental chamber, particularly in a high voltage electron microscope (HVEM). Environmental cells have been used with either windows 20–50 mm apart[2] (allows high water/cement ratios to be examined at 1 atm.), or differential apertures[3] (water pressures are $\leq$ 300 torr). For example, water has been injected into cement and hydration followed at high water:cement (>10:1) ratios and examined using a windowed environmental cell[2]. Used to examine microsilica[4] and slags in cement[5].	If an environmental cell is not used, specimens must be dried out or be well-aged for examination in the high vacuum, which modifies the microstructure. Difficult specimen preparation, using ion-beam thinning: to minimize thermal damage, a cold stage is used and thinning rates kept to < 4 μm h^{-1}. Young pastes must be impregnated with epoxy resin prior to thinning (to hold them together). If the specimens are not examined in an environmental chamber in the TEM, they must be carbon-coated to avoid charging[6]. In environmental cells, windows (which limit resolution as does presence of water) or differential apertures (better resolution) limit resolution. Specimens suffer both thermal and irradiation damage under the electron beam.
Scanning transmission electron microscopy (STEM)	•Conventional –1 nm • With field	A narrow electron probe is rastered over the specimen which is imaged in either transmission of forward-diffracted dark-field mode using a camera and TV system. Has the advantage that both imaging, diffraction and other	Specimen preparation problems are the same as TEM.

[1]H.R. Stewart and J.E. Bailey (1983) *Journal of Materials Science*, **18**: 3686;

K.L. Scrivener and P.L. Pratt (1983) *Materials Research Society Proceedings*, MRS, Pittsburgh vol. 31, p. 351;

R. Javels, J.C. Maso and J.P. Ollivier (1974) *Cement and Concrete Research*, **4**: 167;

R. Javels, J.C. Maso, J.P. Ollivier and B. Thenoz (1975) *Cement and Concrete Research*, **5**: 285;

B.J. Daghleish, P.L. Pratt and R.I. Moss, *Cement and Concrete Research*, **10**: 665;

B.J. Daghleish and K. Ibe, *Cement and Concrete Research*, **11**: 729.

[2]D.D. Double, *Materials Science and Engineering*, **12**: 29;

D.D. Double, A. Hellawell and S.J. Perry (1978) *Proceedings of the Royal Society of London*, vol. A359, p. 435;

[3]H.M. Jennings and P.L. Pratt (1980) *Proceedings of the 7th International Congress on the Chemistry of Cement,* Vol. II, Editions Septima, Paris, p. 141;

K.L. Scrivener and P.L. Pratt (1983) *Materials Research Society Proceedings*, MRS, Pittsburgh, vol. 31, p. 351;

K.L. Scrivener and P.L. Pratt (1984) In *Chemistry and Chemically Related Properties of Cement* (F.P. Glasser, Ed.), *Proceedings of the British Ceramic Society*, Stoke-on-Trent, vol. 35, p. 207.

[4]L.R. Roberts (1989) In *Materials Science of Concrete and Cement* (J. Skalny, Ed.), The American Ceramic Society, Westerville, Ohio, vol I, p. 197.

[5]F.P. Glasser (1989) In *Materials Science of Concrete and Cement* (J. Skalny, Ed.), The American Ceramic Society, Westerville, Ohio, Vol II, 41.

[6]I.G. Richardson and G.W. Groves (1993) *Journal of Materials Science*, **28**: 265.

Technique	Resolution	Advantages	Disadvantages
	emission gun –0.15 nm	microchemical analytical techniques can be used simultaneously (see below). Similar to TEM but generally less radiation damage. A gas reaction cell in a STEM has been used to observe the morphology of C-S-H[7].	
Energy dispersive spectroscopy (EDS) in a TEM/STEM	• Resolution ~ 25 nm • Detection limit ~0.3 wt. % • $Z \geq 5$ detectable best for higher Z	X-ray fluorescence technique in which the elements present are distinguished on the basis of the energies of x-rays that they produce. All elements recorded simultaneously. Atomic number contrast maps can be produced. Small interaction volume. Elements with $Z \geq 5$ detectable but best with heavier elements. Atomic number contrast maps can be produced[8].	Beam damage. Contamination build-up from using a small (10-nm) fixed probe. Specimens can suffer extreme thermal and irradiation damage under the electron beam.
Electron energy loss spectroscopy (EELS) in a TEM/STEM	• Resolution ~ 10 nm • Detection limit ~0.5 wt. % • All elements detectable but best for lower Z	Technique in which the elements present are distinguished on the basis of the energy absorbed (lost) from the transmitted electron beam. Small interaction volume. All elements detectable but best for light elements. Energy filtered images and atomic number contrast maps can be produced. Thus far, does not appear to have been applied to concrete.	Beam damage. Contamination buildup from using a small fixed probe. Specimens can suffer extreme thermal and irradiation damage under the electron beam.
Scanning electron microscopy (SEM)	• Secondary electrons (conventional) –1 nm (with field emission gun) • Backscattered electrons –50–250 nm	An electron beam is rastered over the specimen and either the resulting secondary or backscattered electrons (or for conductors absorbed electrons) are collected and used to form an image on a TV. Large depth of field means that fracture surfaces are easily studied and that surface smoothness is not critical. Secondary electrons (SE) fractography can use to show 3-D arrangement of phases. In older pastes, fracture surface is dominated by areas of cleaved calcium hydroxide. For hydration products of > 1 day difficult to assess how representative are fracture surfaces of bulk microstructure. Backscattered electrons (BSE) needs flat polished specimens (SE give little contrast from such specimens); use atomic number contrast to examine unetched specimens and	Problems with nonconducting nature of cement and the need to dry cement pastes and concrete prior to examination, leading to possible artifacts. Carbon coating of specimens may be needed. In young pastes, fracture surface is interparticular showing only the outer surface of the hydration products. Polishing to produce flat specimens may lead to damage and artifacts.

[7]H.M. Jenning (1980) *Journal of Materials Science,* **15:** 250; H.M. Jennings, B.J. Dalgleish and P.L. Pratt (1981) *Journal of American Ceramics Society* **64:** 567.
[8]I.G. Richardson and G.W. Groves (1993) *Journal of Materials Science,* **28:** 265.

APPENDIX B (CONT'D): IMAGING TECHNIQUES

Technique	Resolution	Advantages	Disadvantages
		distinguish anhydrous material, massive calcium hydroxide, other hydration products, porosity and aggregate particles[9]. Contrast sufficient for image analysis to quantify area and distribution of components[10]. Has the advantage that both imaging, diffraction and other microchemical analytical techniques can be used simultaneously (see below). C-S-H has been observed as spiky outcrops on surfaces of grains[11]. Has been used to examine effect of different minerals in the microstructure, e.g., sand[12], microsilica[13], silica fume[14]. Used to examine the interfacial transition zone around aggregates[15] and other reinforcements such as steel[16] and	

---

[9]K.L. Scrivener and P.L. Pratt (1984) *Proceedings of the 6th International Conference on the Microscopy of Cements*, International Cement Microscopy Association, p. 145.

[10]K.L. Scrivener, H.H. Patel, P.L. Pratt and L.J. Parrott (1987) *Proceedings of the Materials Research Society*, MRS, Pittsburgh, vol. 85, p. 67;

K.L. Scrivener, *Proceedings of the Materials Research Society*, (1987) MRS, Pittsburgh, vol. 85, p. 39;

S.A. Rodger, G.W. Groves, N.J. Clayden and C.M. Dobson (1987) *Proceedings of the Materials Research Society*, MRS, Pittsburgh vol. 85, p. 13;

A.R. Ramachandran and M.W. Grutzech (1987) *Proceedings of the Materials Research Society*, MRS, Pittsburgh, vol. 85, p. 33;

L. Parrott (1987) Proceedings of the Materials Research Society, MRS, Pittsburgh, vol. 85, p. 91.

[11]B. Dagleish, A. Ghose, H.M. Jennings and P.L. Pratt (1982) In *International Conference on Concrete at Early Stages*, vol 1, p. 137;

Y. Halse, P.L. Pratt, J. Daziel and W.A. Gutteridge (1984) In *Chemistry and Chemically Related Properties of Cement,* Edited by F.P. Glasser, Proceedings of the British Ceramic Society, Stoke-on-Trent, vol. 35, p. 403.

[12]M.W. Grutzeck (1987) *Proceedings of the Materials Research Society*, MRS, Pittsburgh, vol. 85, p. 55.

[13]M. Regourd, in *Condensed Silica Fume* (P.C. Aitcin, Ed.) Les Editions de l'Universite de Sherbrooke, Quebec, Canada, p. 20;

P.C. Aitcin, M. Regourd and C. Bedard (1983) *Proceedings of the 5th International Conference on Cement Microscopy, International Cement Microscopy Association, Duncanville, Texas*, 1983164;

Chen Zhi-Yuan and Zhang Xio-Zhong (1986) *Proceedings of the 8th International Congress on the Chemistry of Cement*, Finep, Rio de Janeiro, Brazil, Vol. III, p. 450;

Chen Zhi-Yuan and I. Odler (1987) *Cement and Concrete Research,* **17**: 784;

J.P. Ollivier (1986) *Proceedings of the 8th International Congress on the Chemistry of Cement,* Finep, Rio de Janeiro, Brazil, vol. VI, p. 189;

P.J.M. Monteiro and P.K. Mehta (1986) *Proceedings of the 8th International Congress on the Chemistry of Cement*, Vol. III, Finep, Rio de Janeiro, Brazil, 433;

Wang Jia, Liu Baoyuan, Xie Songshan and Wu Zhongwei, *Proceedings of the 8th International Congress on the Chemistry of Cement,* Vol. III, Finep, Rio de Janeiro, Brazil, (1986) 460;

M. Regourd (1985) *Proceedings of the Materials Research Society*, MRS, Pittsburgh, vol. 42, p.3;

K.L. Scrivener, K.D. Baldie, Y. Halse and P.L. Pratt (1985) *Proceedings of the Materials Research Society*, MRS, Pittsburgh,vol. 42 p. 39;

M.J. Scali, D. Chin and N.S. Berke (1987) *Proceedings of the 9th International Conference on Cement Microscopy*, International Cement Microscopy Association, Duncanville, Texas, p.375.

[14]K.L. Scrivener, and A. Bentur (1988) *Advances in Cement Research,* 1[4]: 230.

[15]K.L. Scrivener and P.L. Pratt (1986) In *Proceedings of the 8th International Congress on the Chemistry of Cement*, vol. III, Finep, Rio de Janeiro, Brazil, (1986) 466;

K.L. Scrivener and E.M. Gartner, *Proceedings of the Materials Research Society,* MRS, Pittsburgh, vol. 85;

K.L. Scrivener (1987) *Proceedings of the Materials Research Society,* MRS, Pittsburgh, vol. 85 p. 39.

A. Bentur, A. Goldman and M.D. Cohen (1988) *Materials Research Society Proceedings,* MRS, Pittsburgh, vol. 114, 97.

[16]A. Bentur, S. Diamond and S. Mindess (1985) *Journal of Materials Science,* **20:** 3610.

APPENDIX B (CONT'D): IMAGING TECHNIQUES

Technique	Resolution	Advantages	Disadvantages
		glass[17]. Can be used to examine fine pores either by direct observation of thin or sectioned specimens[18]. The volumes obtained were consistent with those obtained by butane adsorption for pores greater than 50 nm.	
Energy dispersive spectroscopy (EDS) in a SEM	• ~ 1 μm • Detection limit ~ 0.3 wt. % • $Z \geq 5$ detectable best at higher Z.	X-ray fluorescence technique in which elements are distinguished on the basis of the energies of x-rays that they produce. All elements recorded simultaneously. Atomic number contrast maps can be produced which combined with BSE images (see above) can give information on proportions of phases and distribution[19] and can be used to examine components, e.g. sand[20] or slag containing cement[21]. Can be used to examine pores on sectioned specimens by infiltrating with a polymer containing an element which is readily detected by EDS, e.g., chlorine, and performing dot mapping (areal analysis)[22].	Large interaction volume of electron beam means that information comes from a volume of ~ 1 μm³. The time (~100 s) needed for the focused probe to remain on a given area causes significant local damage to cement specimens. See problems associated with the SEM. For pore observation, limited by the ability to infiltrate the polymer (resolution 3-5 μm).
Wavelength dispersive spectroscopy (WDS) in a SEM	• ~ 1 μm • Detection limit ~0.1 wt. % • $Z \geq 3$ measurable	X-ray fluorescence technique in which elements are distinguished on the basis of the wavelengths of x-rays that they produce. Better statistics than EDS (less noise). Atomic number contrast maps can be produced which combined with BSE images can give information on proportions of phases and distribution. The electron probe microanalyzer (EPMA) uses several spectrometers at once and, thus, can record the x-rays from several (typically, up to 4) elements at once. Appears not to have been used on cement and concrete.	Large interaction volume of electron beam means that information comes from a volume of ~ 1 μm³. Since x-rays from a number of elements are recorded serially rather than simultaneously, if the specimen chemistry is changing with time this may lead to problems. The time (~100 s) needed for the focused probe to remain on a given area causes significant local damage to cement specimens. See problems associated with the SEM.

[17]A. Bentur (1986) In *Proceedings of the Symposium on the Durability of Glass-Fiber Reinforced Cement,* (S. Diamond, Ed.) Prestressed Concrete Institute, Chicago, p. 109;

[18]L.J. Parrott, R.G. Patel, D.C. Killoh and H.M. Jennings (1984) *Journal of American Ceramic Society,* **67:** 233.

[19]K.L. Scrivener (1987) *Proceedings of the Materials Research Society,* MRS, Pittsburgh, vol. 85, p. 39;
M. Regourd (1987) *Proceedings of the Materials Research Society,* MRS, Pittsburgh vol. 85, p. 187.

[20]M.W. Grutzeck (1987) *Proceedings of the Materials Research Society,* MRS, Pittsburgh, vol. 85, p. 55.

[21]A.M. Harrisson, N.B. Winter and H.F.W. Taylor (1987) *Proceedings of the Materials Research Society*, MRS, Pittsburgh, vol. 85, p.213.

[22]P.W. Brown, D. Shi and J. Skalny (1989) In *Materials Science of Concrete and Cement* (J. Skalny, Ed.) Vol II, The American Ceramic Society, Westerville, Ohio, 83;
S. Lee, D.M. Roy and R.I.A. Malek (1987) *Proceedings of the Materials Research Society,* MRS, Pittsburgh, vol. 85, p. 273.

APPENDIX B (CONT'D): IMAGING TECHNIQUES

Technique	Resolution	Advantages	Disadvantages
Electron back-scattered patterns (EBSP) in a SEM	• Smallest dia. - 1 μm • Angular resolution - 0.05˚	A stationary probe on the specimen produces a diffraction pattern using backscattered electrons which can be used to identify phases and their orientation. (Replaces the older channeling pattern technique.) Thus far, does not appear to have been applied to concrete.	Putting the focused probe onto a single area for the 1 second required may cause local damage to cement specimens. See problems associated with the SEM.
Environmental scanning electron microscopy (ESSEM)	• 3.5 nm (high vac.) • 5.5 nm (low vac.)	A commercially available modification of a standard SEM. Can examine concrete in "wet" condition, i.e. operates at water vapor pressures 6–270 Pa in low vac mode. No need to coat specimen since gases in chamber are ionized and prevent charging. EDS as for conventional SEM. Use of BSE electrons allows atomic contrast imaging (need flat specimen for this). Large depth of field. ESEM used to examine the hydration of C3S[23] including use of EDS. A Peltier cell has been used to cool the specimen and, thus, maintain a low water vapor pressure when water was injected into the cement in-situ[24]. BSE in the ESEM used to examine the transition zone[25].	A little lower resolution than conventional SEM.
Scanning acoustic microscopy	• 1 mm (1 GHz) • 15 mm (100 MHz)	A "beam" of acoustic waves is rastered over the specimen and reflected waves are used to produce an image (on a TV screen) of differences in acoustic impedance. Water is normally used as the coupling medium; thus, concrete is examined in wet condition. Can image below surface: 15-20 μm at 1 GHz, ~10 mm at 100 MHz, allowing serial sectioning. Can observe water-filled voids as small as 1 μm (at 1 GHz) but image will appear larger than this. Can clearly observe transition zone[26]. Could examine freeze/thaw behavior using glycerin or another oil as coupling fluid with only slight degradation in resolution. Fringes from Rayleigh waves show the presence	Small depth of field in high resolution mode (1 GHz) means that surface has to be polished to better than ~ 0.5 μm. Such polishing is very difficult for concrete without pull-out of different phases. There is some possibility that polishing may produce artifacts. This may be checked in the low resolution mode (100 MHz) by comparing surface or near-surface images with images from well-below the surface. Any damage or artifact problem is likely to be more serious when the

---

[23]TB. Bergstrom and H.M. Jennings (1992) *Journal of Materials Science,* **11:** 620;
P. Meredith, A.M. Donald and K. Luke (1995) *Journal of Materials Science,* **30:** 1921.
[24]D.A. Lange, K. Sujata and H.M. Jennings (1992) *Ultramicroscopy,* **37:** 234.
[25]A.W. Pope and H.M. Jennings (1992) *Journal of Materials Science* **27:** 6452.
[26]M.H. Manghnani and R.A. Livingston (1995) unpublished.

Technique	Resolution	Advantages	Disadvantages
		of inclined or vertical subsurface cracks < 100 nm. Can be used to observe large pores in sectioned specimens.	instrument is used in the high resolution configuration (1 GHz).
Scanning electron (scanning laser) acoustic microscopy	• 0.1–0.3 mm	An electron beam (in a SEM) is chopped at frequencies in the range 100 kHz to 5 MHz, which produces periodic heating in the specimen. The resulting damped thermal wave excites an acoustic wave which can be picked up by a piezoelectric crystal transducer under the specimen. A related approach uses a laser to produce the thermal wave. Thus far, it does not appear to have been applied to concrete.	Probably similar limitations to a scanning acoustic microscope. Also has some of the problems associated with the SEM or ESEM in which it is performed.
Scanning force microscopy (SFM or AFM)	• 0.001 nm vertical • 10 nm lateral	A fine probe (sharp tip) is scanned over the surface and differences in topography are recorded from variations in the displacement of the probe needed to maintain a constant force. Can operate in air or liquid, and the material can be a conductor or nonconductor. Can measure electrical or magnetic forces. Thus far, does not appear to have been applied to concrete. The polarization force between an electrically charged AFM tip and a substrate has been used to follow the condensation and evaporation of a monolayer of water on mica at room temperature[27]. It is possible that the same technique could be applied to concrete if a flat enough surface could be obtained.	Some artifacts occur during imaging. Requires flat surface < 10 μm to operate. For atomic level resolution needs an atomically flat surface. Probably difficult to use for concrete because of the difficulty of surface preparation.
Scanning capacitance microscopy (SCM)	• 100 nm • ~ 3 x electronic charge	A fine probe (sharp tip) is scanned over the surface and differences in topography are recorded from variations in the capacitance. The local electrical conductivity can also be measured. Thus far, does not appear to have been applied to concrete.	Some artifacts occur during imaging. Requires flat surface < 10 μm to operate. Probably difficult to use for concrete because of the difficulty of surface preparation.
Scanning tunneling microscopy (STM)	• 0.01 nm	A fine probe (sharp tip) is scanned over the surface and differences in topography are recorded from variations in the measured tunneling current. Atomic number contrast is also possible on atomically flat specimens. Thus, both individual	Some artifacts occur during imaging. Requires flat surface < 10 μm to operate. Probably inapplicable to cement and concrete since the material has to be a conductor or

[27]J. Hu, X.-D. Xiao, D.F. Ogletree and M. Salmeron (1995) *Science*, 268, April, 267;

APPENDIX B (CONT'D): IMAGING TECHNIQUES

Technique	Resolution	Advantages	Disadvantages
		phases and atoms can be imaged. Thus far, does not appear to have been applied to concrete.	semiconductor.
Optical microscopy	• 1 μm	Uses reflected or transmitted light to image phases. Etchants can be used to study distribution of anhydrous phases in clinker and cement powder quantitatively[28]. In thin sections of hydrated pastes and concrete, refractive properties of different phases and use of fluorescent resin can indicate cement and aggregate type, the W/C ratio, the presence of mineral admixtures, the quality of compaction and the presence of alkali silica reaction[29]. A standard technique for cement and concrete. Can be used to observe large pores[30] in polished or thin sectioned specimens and microcracks[31], a technique which is enhanced by the use of ordinary or fluorescent dyes. Serial sectioning can be used to obtain the three-dimensional distribution.	Small depth of field. Poor resolution. Hydrated pastes and concrete little contrast in reflected light. There is some possibility that polishing can cause structural changes in the surface and, hence, artifacts. Since only the surface is viewed, polishing to produce a flat surface may cause damage and artifacts, and pull out phases in concrete.
(Laser scanning) confocal optical microscopy	• 1 μm	Scans an optical light beam over a specimen and records the reflected or transmitted intensity as an image on a TV screen. Can examine concrete in either wet or dry condition. Contrast modes as for OM. Thus far, does not appear to have been applied to concrete.	Individual images have less depth of field than conventional OM but can vertically scan through images to give 3-D picture. Resolution as for OM.

[28]G.R. Long (1982) In *Characterization and Performance Prediction of Cement and Concrete* (J.F. Young, Ed.) Engineering Foundation, New York, p. 39;
E. Fundal, FLS Review, no. 25, FL Smidth, Copenhagen.
[29]N. Thaulow, A. Damgaard Jensen, S. Chatterji, P. Christensen and H. Gudmundsson (1982) *Nordisk Betong*, **2-4**: 51.
H.N. Walker and B.F. Marshall, *Cement and Concrete Aggregates*, **1**: 3.
[30]G.V. Chilingarian, C.Y. Zhang, M.Y. Al-Bassam and T.F. Yen (1986) *Energy Resources*, **8**: 369;
C. Straley and M.M. Minnis (1983) *Journal of Sedimentary Petrology*, **53**: 667.
[31]L. Knab, H. Walker, J. Clifton and E. Fuller (1984) *Cement and Concrete Research*, **14**: 339.

APPENDIX C: INDIRECT TECHNIQUES

Technique	Resolution	Advantages	Disadvantages
X-ray diffraction (XRD)	• ~ 1 wt % using standards	Can examine concrete in either wet or dry condition. Identify crystalline phases and determine amounts to within 1% (in clinker) if standards are used on a conventional x-ray set[1]. Can be used to follow hydration[2]. Synchrotron radiation improves detection limits and resolution (0.03°) of measurements. Can also be used to examine aggregates such as microsilica[3] and slags[4]. The orientation of calcium hydroxide crystals in the transition zone can be determined by casting cement pastes against polished surfaces[5] although this approach has been questioned[6]. *Synchrotron radiation appears not to have been used for this purpose.*	A conventional x-ray set is not particularly useful for following hydration reactions since good quality data take at least 1 hr to acquire. A synchrotron source would allow hydration to be studied over small (few seconds) time steps. Very thin specimens are needed due to the large absorption of x-rays. The use of thin specimens raises questions about the validity of the data which, is from near the specimen surface, where carbonation or dehydration may have occurred. Since the specimens need to be flat, polishing can lead to artifacts and damage. Not particularly useful for non-crystalline materials.
Neutron diffraction	• ~ 1 wt % using standards	Similar to x-ray diffraction but neutrons are scattered much more strongly from some light atoms, e.g., H, than x-rays. Also, since neutrons are much more penetrating than x-rays thicker specimens can be used. Used to study the development of hydrous phases in cement as a function of time[7].	The main problem is that the technique requires access to a high intensity neutron source. Similar specimen difficulties to x-ray diffraction.
X-ray photoelectron spectrometry (XPS), also called ESCA	• spatial ~1 μm • depth ~2 nm • detection –1% • Z > 1 • composition ± 5%	An x-ray source (1 keV) illuminates the specimen in an ultra high vacuum, UHV, $(1 \times 10^{-8}$ Pa), and both photoelectrons and auger electrons from the specimen are captured and recorded as counts versus energy. The photoelectron peaks are characteristic of the core electron levels, giving composition	The two major problems are that only the surface is probed, and that the UHV will lead to rapid drying of the specimen, if it has not been dried already.

[1]L. Stuble (1983) In *Characterization and Performance of Cement and Concrete,* Engineering Foundation, New York, p. 31;
W.A. Gutteridge (1984) *Chemistry and Chemically Related Properties of Cement, Proceedings of the British Ceramic Society*, Stoke-on-Trent, Vol. 35, p.11;
J. Grandet, and J.P. Ollivier (1980) *Proceedings of the 7th International Congress on the Chemistry of Cement,* Vol. III, Editions Septima, Paris, p .63;
[2]H.Y. Ghorab, and S.H.A. El Fetouh (1987) *Proceedings of the Materials Research Society*, Vol. 85, MRS, Pittsburgh, p. 255.
[3]P.C. Aitcin, A. Carles-Gibergues, M.N. Oudjit, and A. Vaquier (1986) *Proceedings of the 8th International Congress on the Chemistry of Cement*, Vol IV, Finep, Rio de Janeiro, Brazil, p. 27.
[4]A.M. Harrisson, N.B. Winter, and H.F.W. Taylor (1987) *Proceedings of the Materials Research Society*, Vol. 85, MRS, Pittsburgh, p. 213.
[5]J.C. Maso (1980) *Proceedings of the 7th International Congress on the Chemistry of Cement*, Editions Septima, Paris, Vol I, p. VII-1/3-VII-1/15.
[6]K.L. Scrivener, and E.M. Gartner (1987) *Proceedings of the Materials Research Society Proceedings*, MRS, Pittsburgh, Vol. 85;
[7]R.A. Livingston, D.A. Neumann, A. Allen, and J.J. Rush (1995) *Proceedings of the Materials Research Society*.

Technique	Resolution	Advantages	Disadvantages
		information, and shifts in the peaks give information about chemical bonding. Sputter depth profiling is possible but slow and with the problem that not all atomic species are sputtered at the same rate. Has been used to show that only a thin layer of C_3S is hydrated at early ages[8].	
Auger electron spectroscopy (AES)	• resolution –0.1 μm • detection limit –0.1% • Z > 2 • depth –1 nm	Electrons at 0.2–2 keV illuminate the specimen in an ultra high vacuum (1×10^{-8} Pa) and the emitted Auger electrons are captured and recorded as counts versus energy. These emitted electrons are characteristic of the outer electron energy levels, giving compositional information. Sputter depth profiling is possible but slow and with the problem that not all atomic species are sputtered at the same rate. *Thus far, appears not to have been applied to the study of cement or concrete.*	The two major problems are that only the surface is probed, and that the UHV will lead to rapid drying of the specimen, if it has not been dried already.
Secondary ion mass spectroscopy (SIMS)	• low energy beams, resolution –0.1 μm • detection limit ~0.1 ppm • depth < 1 μm • Z ≥ 1	An ion beam (energy 100 eV–100 keV), produced from H, He, Xe or Ar gas, is rastered over the specimen in a vacuum of 10^{-3}–10^{-4} Pa. Ions sputtered from the surface are analyzed on the basis of their mass. An image can be formed at the same time, typically using secondary electrons. With a low accelerating voltage and light (H) ions, information from only the top one or two atom layers is possible. With heavy ions and higher accelerating voltages, depth profiling can be performed. Used to show that surface of cement grains may contain a high proportion of impurities, which may affect reactivity[9].	The two major problems are that only the surface is probed, and that the vacuum will lead to rapid drying of the specimen, if it has not been dried already.
Raman spectroscopy	• time resolution < 1 min • quantification of	Light from a laser (typically green, 514.5 nm) is used to excite the specimen, and the resulting spectra are recorded as intensity versus wavenumber (typically 1300–100 cm^{-1}).	Light only penetrates the outermost layer of the specimen. Thus, data are susceptible to surface contamination or carbonation. Only

[8]M. Regourd (1983) *Philosophical Transactions of the Royal Society of London*, **A310:** 85.
[9]W. Gerhard, and E. Nagele (1983) *Cement and Concrete Research*, **13**: 846.

APPENDIX C (CONT'D): INDIRECT TECHNIQUES

Technique	Resolution	Advantages	Disadvantages
	phase amounts: 2–10%	Can be performed in-situ using a fiber probe. Characteristic peaks or groups of peaks are associated with bending, e.g. of O-Si-O, or stretching, e.g. of Si-O, modes of various bonds. The intensity of a peak indicates the numbers of these bonds, and hence the phases present. The technique is non-invasive and can be used to study hydration of cement-based materials as a function of time[10].	gives information on phases present not on other aspects of the structure, e.g., pores and free or bound water.
Rutherford backscattering spectrometry (RBS)	• resolution: 1–3 mm • depth < 10 mm • composition ± 1% • detection: 0.1% • Z > 4	High energy (100 keV-1 MeV) He$^+$ ion beam (spot size- 2 mm^2) scattered elastically off ions in the specimen, give a plot of intensity vs. backscattered angle. This provides accurate information on the number per unit area for the elements present. Line shape analysis, and use of different bombarding ions can provide depth profiles of certain elements. *Thus far, appears not to have been applied to the study of cement or concrete.*	Requires thin specimens for good resolution, leading to specimen preparation difficulties. Confined to near-surface region. Thus, data are suceptible to surface contamination or carbonation. Must be performed in a vacuum, which will lead to rapid drying of the specimen, if it has not been dried already.
Ignition		Standard technique used to determine evaporable water by drying to constant weight at around 110°C and then igniting at around 1050°C[11]. Porosity can be calculated on the basis that the evaporable water filled all the pores.	Closed pores do not allow the water to escape.
Permeability methods		Standard techniques used to give surface area of cement grains and microsilica particle size. Both total porosity and its distribution determine the permeability, but only pores greater than a specific value contribute to the permeability[12]. The most common technique is measurement	These methods give lower surface areas than absorption methods due to blocked channels not accessible to moving air/fluid streams[14]. May give size of agglomerate rather than individual particle size.

[10]M. Tarrida, M. Madon, B. Le Rolland, and P. Colombet (1995) *Advances in Cement Based Materials*, **2:** 15.

[11]R.H. Mills, and N. Buenfeld (1987) *Proceedings of the Materials Research Society*, Vol. 85, MRS, Pittsburgh, p.235.

[12]B.K. Nyame, and J.M. Illston (1980) *7th International Congress on the Chemistry of Cement,* **3**: VI-181;

P.K. Mehta, and D. Manmohan (1985) *7th International Congress on the Chemistry of Cement,* **3**: VII-1.

D.C. Hughes, *Magazine of Concrete Research*, **37:** 227;

S. Goto and D.M. Roy, *Cement and Concrete Research*, **11** (1981) 575;

P.W. Brown, D. Shi, and J. Skalny (1989) In *Materials Science of Concrete and Cement*, J. Skalny, Ed., Vol II, The American Ceramic Society, Westerville, Ohio, p.127.

APPENDIX C (CONT'D): INDIRECT TECHNIQUES

Technique	Resolution	Advantages	Disadvantages
		of the amount of water that can be forced into the specimen under a large hydraulic head. The rapid chloride permeability method is also common, in which chloride ions are migrated through the specimen under a potential gradient[13]—useful since rapid.	Specific problems with water techniques: for impermeable specimens, small specimens have to be used which can lead to problems with lack of representativeness; since solubilities of phases vary with local hydrostatic pressure, pressure gradients through the specimen can lead to phase redistribution, which affects the pore structure and permeability; specimens with low permeabilities are difficult to saturate (problem with all permeability methods). Disadvantage of chloride method is that the potential across the specimen causes heating; and the chloride can react with aluminate phases. In order to relate permeability to porosity a model must be used and these are also a source of error.
Mercury intrusion porosimetry (MIP)[15]	• pore size range 2 nm to > 2 mm	For many years, primary method for investigating pore-size distribution of hardened cement paste. Based on idea that mercury will not wet most surfaces and must be forced in to pores with pressure, P, given by the Washburn equation $r = -2\gamma \cos \theta / P$, where γ is the surface tension of mercury and θ is the contact angle (usually 130–140°). The sample is evacuated, surrounded with mercury and the volume change measured as the pressure is increased (from sub-ambient to 400 MPa). Pioneered by Winslow and Diamond[16]. Advantages: rapid, automated analysis; high volume resolution. Can obtain total porosity, capillary porosity and gel porosity. Best for pores in the range 3.5 nm to 200	No information on pore spatial distribution. Disadvantages: specimen needs to be dried causing damage and different pore sizes depending on the drying technique; contact angle and surface tension uncertainty; inability to probe microporosity (pore diameter < 2 nm); sample compression from high pressures; destruction of the sample; need to dry the sample; network/percolation effects "ink-bottle effect" (since a larger pore may be filled with mercury via a smaller pore, this biases data to smaller

[13]D. Whiting (1981) FHWA Report RD-81/119, Federal Highway Administration, Washington, D.C.

[14]K. Scrivener (1980) In *Materials Science of Concrete and Cement* (J. Skalny, Ed.), Vol I, The International Congress on the Chemistry of Cement, vol. 3, p. VII-1;

[15]D.M. Smith, D.-W. Hua, and W.L. Earl (1994) *Materials Research Society Bulletin*, April, **44**.

[16]D. Winslow, and S. Diamond (1970) *Journal of Materials Research*, **5**, p. 564.

D. Winslow, and C.W. Lovell (1981) *Powder Technology*, **29:** 151.

Technique	Resolution	Advantages	Disadvantages
		mm. Gives the same result as helium pyncometry for plain dried pastes but in blended pastes MIP gives higher porosities[17]. (Different drying techniques also give different porosities using the helium technique.) Also used for the study of fly ash and microsilica pastes[18].	pore sizes)[19]. Structure can be altered during mercury intrusion. For pore sizes in the range 50–100 nm capillary desiccation is important and drying at < 105°C can lead to incomplete dry ing. Closed porosity is not intruded, but since this will not contribute to transport processes this may not be a problem.
Gas (nitrogen) adsorption[20]	• well-established for mesoporous solids, i.e. pore diameters 2–50 nm	Surface area of silica particles measured by this technique correlates well with TEM measurements due to lack of significant internal surface[21]. Typically, performed using the Brunauer, Emmett and Teller (BET) approach which allows for multilayer adsorption. The data (Volume, V, vs. P/P_o, where P_o is the saturation pressure) are plotted in a linear form in the range 0.05–0.3: $1/V(P_o/P-1)) = 1/(V_m C) + (C-1)/(V_m C)P/P_o$ V_m and C are extracted from the slope and intercept. $V_m \cdot C$ is a measure of the adsorbent-adsorbate interactions. Used to measure pore structure of cement in the range 0.35 nm to 70 nm[22].	At larger pressures hysteresis may be observed on adsorption and desorption. For microporous solids (pore diameter < 2 nm) the equation shown left may not hold. Can alter the structure during gas intrusion. Internal areas determined by gas adsorption are dominated by gel porosity which have only a minor effect on bulk transport.

40

[17]B.K. Marsh, and R.L. Day (1985) *Materials Research Society Proceedings, Pittsburgh,* Vol. 42 p. 113;

[18]A. Durekovic (1986) *8th International Congress on the Chemistry of Cement,* Vol IV, Finep, Rio de Janeiro, Brazil;

P.C. Aitcin, M. Regourd, and C. Bedard (1983) *Proceedings of the 5th International Conference on Cement Microscopy Association, Duncanville, Texas*, p. 164;

R.F. Feldman, and H. Cheng-yi (1985) *Cement and Concrete Research*, **15**: 285.

R.F. Feldman (1986) *Cement and Concrete Research*, **16**: 31;

M. Buil, and P. Delage (1987) *Cement and Concrete Research*, **17**: 65;

B.K. Marsh, R.C. Joshi, and A. Balasundaram (1987) *Proceedings of the Materials Research Society, Pittsburgh,* Vol. 85, p.61;

Th. A. Bier (1987) *Proceedings of the Materials Research Society, Pittsburgh,* Vol. 85, p. 123;

D.J. Cook, H.T. Cao, and E.P. Coan (1987) *Proceedings of the Materials Research Society, Pittsburgh*, Vol. 85, p.201.

[19]R.F. Feldman (1986) *8th International Congress on the Chemistry of Cement*, Vol I, Finep, Rio de Janeiro, Brazil, p337;

D. Manmohan, and P.K. Mehta (1981) *Cement and Concrete Aggregates*, **3**: 63;

P. Parceveaux (1984) *Cement and Concrete Research*, **14**: 419.

[20]D.M. Smith, D.-W. Hua, and W.L. Earl (1994) *Materials Research Society Bulletin,* April, p. 44.

[21]G. Rau, and P.C. Aitcin (1983) In *Condensed Silica Fume*, P.C. Aitcin, Ed., Les Editions de l'Universite de Sherbrooke, Quebec, Canada, p. 9;

P.C. Aitcin, P. Pinsonneault, and D.M. Roy (1984) American Ceramic Society Bulletin, **63**: 1487;

P.C. Aitcin, A. Carles-Gibergues, M.N. Oudjit, and A. Vaquier (1986) *8th International Congress on the Chemistry of Cement*, Vol. IV, Finep, Rio de Janeiro, Brazil, p. 27

[22]W. Hansen, and J. Almudaiheem (1987) *Proceedings of the Materials Research Society*, Vol. 85, MRS, Pittsburgh, p. 105.

Technique	Resolution	Advantages	Disadvantages
Methanol adsorption		Used to measure pore-size distribution	No information on pore spatial distribution. Fundamental flaw with technique: large pores with small openings will be intruded at pressure corresponding to the entrance of the pore. Thus, measured pore size is larger than (or equal to) calculated pore-size. For cement pastes, pore-size distributions are characterized by threshold pore size—related to interconnectivity of the pores (effect decreases with increasing hydration).
Water adsorption		Similar to nitrogen adsorption except that since water is a polar molecule and adsorbs differently, different results are obtained.	cf. nitrogen adsorption
Nuclear magnetic resonance (NMR)[23]	• peak position –0.01 ppm of a applied field	This technique probes the (spin) quantization of the magnetic moments of some nuclei in a magnetic field by pulsing in the radio frequency range (say 30–90 MHz). The resonance that occurs between the applied field and the specimen is sensitive to the local environment of the nucleus. The quantities measured are the relaxation times (nuclear spin-lattice relaxation time, which is related to the crystal structure of hydrates or the mobility of the water, and the spin-spin relaxation time which indicates the dynamic state of the water) and the peak position or chemical shift, which is very sensitive to local environment or bonding. Proton NMR distinguishes between free water and adsorbed or combined water[24]. Both proton NMR and solid state NMR with ^{29}Si and ^{27}Al have been used to follow hydration of silicates and aluminates and to study the effects of accelerators, retarders and superplasticizers on the hydration of cement minerals[25]. Has the advantage that specimens do not have to be dried.	For some materials, NMR has been used to characterize pore structure. This effect arises because water near the pore walls have more mechanisms for relaxation than those in the center of the pore and have shorter relaxation times. However, there is no consensus on the mathematical formalism relating NMR measurements to pore size distribution.

[23]D.M. Smith, D.-W. Hua, and W.L. Earl (1994) *Materials Research Society Bulletin*, April, **44**.
[24]M. Regourd (1987) *Proceedings of the Materials Research Society*, Vol. 85, MRS, Pittsburgh, p. 245.
[25]S.A. Rodger, G.W. Groves, N.J. Clayden, and C.M. Dobson (1987) *Proceedings of the Materials Research Society*, Vol. 85, MRS, Pittsburgh, p. 13.

APPENDIX C (CONT'D): INDIRECT TECHNIQUES

Technique	Resolution	Advantages	Disadvantages
Small angle neutron scattering (SANS)	• using scattering vector range of 0.012–1.5 nm^{-1}, scattering centers ranging from 5 nm to 150 nm can be studied;	Useful for characterizing (using the scattering vector, which is the difference between the incident and scattered wave vectors) the surface and fractal dimensions of the gel (the main scattering phase) as a function of both time and additions such as fly ash and silica fume and for characterizing silica aggregates for potential deleterious reactions in alkaline cements[26]. Volume fractions of 10^{-6} can be detected. Does not require drying of the specimens.	Requires access to a high intensity neutron source. Specimens must be < 1 mm thick to avoid multiple scattering. These thin specimens are difficult to prepare from concrete due to differential phase polishing and phase pull-out but preparation of cement specimens has been demonstrated. Carbonation can occur rapidly in these specimens requiring the use of a CO_2-free atmosphere. Each datum point can take considerable time to acquire depending on the specimen thickness and intensity of the neutron flux, times 0.15–1 hr are typical.
Small angle X-ray scattering (SAXS)		Similar to SANS, useful for characterizing (using the scattering vector, which is the difference between the incident and scattered wave vectors which depends on the abrupt change in electron density at the interface between two phases) the surface and fractal dimensions. Scattering is from both C_2S and C_3S (as for neutrons) and C_3A. Useful for characterizing pore size distributions[27]. Does not require drying of the specimen.	Major limitation is that both x-ray scattering and absorption are ~ 10 times that of neutrons. Thus, very thin (~100 μm) specimens are required otherwise a poor statistics and multiple scattering are obtained making the data difficult to interpret.
Quasi-elastic neutron scattering		Probes the major dynamic modes of motion which characterize the state of the water molecule, i.e., free water has translational, vibrational and rotational freedom; water in C-S-H can vibrate and rotate; whereas the OH- group can only vibrate. The neutron scattering in hydrated cement is dominated by hydrogen and hence these different modes can be probed. The technique can be used to follow nondestructively the hydration of cement and to determine the distribution of water among various states,	Requires access to a high intensity neutron source. Specimens must be < 1 mm thick to avoid multiple scattering. These thin specimens are difficult to prepare from concrete. Carbonation can occur rapidly in these specimens requiring the use of a CO_2-free atmosphere. Currently, it takes 1–2 hr to acquire a single datum point, thus seriously limiting the time resolution. The

[26]R.A. Livingston, D.A. Neumann, A. Allen, and J.J. Rush (1995) *Proceedings of the Materials Research Society*;
A.J. Allen, R.C. Oberthur, D. Pearson, P. Schofield and C.R. Wilding (1987) *Philosophical Magazine,* **56**: 263.
[27]J. Kropp, T. Grafenecker, and H. Hisdorf (1983) *Proceedings of the Symposium on Principles and Applications of Pore Structural Characterization (RILAM), Milan,* p. 83.

APPENDIX C (CONT'D): INDIRECT TECHNIQUES

Technique	Resolution	Advantages	Disadvantages
		i.e., free, chemically-bound or physically trapped and to investigate the formation of ice in pores[28].	technique does not distinguish between adsorbed water and water trapped in gel pores, or between free water in capillary pores and larger pores.
Impedance spectroscopy	• time resolution < 1 min	Measures the electrical impedance (cement is conductive because of the interconnected pore network containing mobile ions), over a range of frequencies, typically 5 Hz-13 MHz but has been extended to 1 GHz[29]. Results are plotted as real versus imaginary impedance, and related to circuit components (Nyquist plot). Can be used to follow structural evolution noninvasively as a function of time[30]. Since the relative dielectric constant is linearly related to the water/cement ratio from 50 MHz to 1 GHz, provides a rapid method of determining the water/cement ratio in a hardened paste.	Indirect determination of structural evolution which has to be correlated with other techniques. Difficult to interpret results in terms of structural changes, and difficult to differentiate between contributions of factors leading to conduction, i.e., ion concentration, water content, pore structure. Models are required to relate the microstructure to the electrical impedance.
Calorimetry		Used to identify various stages of the reaction of cement with water via the heat output[31]. Low temperature calorimetry or differential scanning calorimetry can be used to assess the pore structure. The heat change indicates the amount of water and the temperature indicates the water-	If different reactions are occurring simultaneously it may be very difficult to separate them. The low-temperature calorimetry technique works better for larger pores.

[28]R.A. Livingston, D.A. Neumann, A. Allen, and J.J. Rush (1995) *Proceedings, Materials Research Society*;
D.H.C. Harris, C.G. Windsor, and C.D. Lawrence (1974) *Magazine of Concrete Research*, **26**: 65.
[29]P. Gu, and J.J. Beaudoin (1996) *Journal of Materials Science,* **15**, 182.
[30]W.J. McCarter, S. Garvin, and N. Bouzid (1988) *Journal of Materials Science Letters*, **7**, 1056;
C.A. Scuderi, T.O. Mason, and H.M. Jennings (1991) *Journal of Materials Science*, **26**: 349
[31]P. Gu, and J.J. Beaudoin (1995) *Journal of Materials Science Letters*, **14**: 1207;
H.R. Stewart, and J.E. Bailey (1983) *Journal of Materials Science*, **18**: 3686;
P.W. Brown, C.L. Harner, and E.J. Prosen (1985) *Cement and Concrete Research,* **16:** 17.
K.L. Scrivener (1987) *Materials Research Society Proceedings*, Vol. 85, MRS, Pittsburgh, p. 39;
P.L. Pratt, and A. Ghose (1983) *Philosophical Transactions of the Royal Society of London*, **A 310**: 93;
M. Fukuhara (1977) *Cement and Concrete Research*, **11**: 407;
R. E. Philleo (1989) In *Materials Science of Concrete and Cement*, Edited by J. Skalny, Vol II, The American Ceramic Society, Westerville, Ohio, 1;
H. Uchikawa (1986) *Proceedings of the 8th International Congress on the Chemistry of Cement*, Vol II, Finep, Rio de Janeiro, Brazil, p. 256;
F.P. Glasser, S. Diamond and D.M. Roy (1987) *Proceedings of the Materials Research Society*, Vol. 85, MRS, Pittsburgh, 167.

Technique	Resolution	Advantages	Disadvantages
		filled pore diameter—the smaller the pore the lower the freezing temperature[32]. The technique avoids specimen pre-drying and can be used several times, i.e., frozen and unfrozen, to give similar results.	
Elastic modules measurements		By using mathematical models, based on rule-of-mixtures approach, the volume fractions of components can be determined by knowing the elastic modulus of the components and determining the elastic modulus using dynamic (oscillation) methods[33]. By cooling the specimen, the freezing of water in pores can be followed and since water freezes in small pores at a lower temperature than in large pores, the pore size distribution can be determined. Ice damage can also be followed directly.	Dynamic elastic modulus measurements require that the specimen is in a vacuum chamber so that the oscillations of the specimen after it is struck with a hammer are not damped out by air.
Nanoindenter	• depth penetration –5 nm • lateral resolution –5 to 10 × depth	Essentially a very small, instrumented hardness indenter that provides mechanical properties data (load vs. depth of indentation) on a very fine scale. Thus far, does not appear to have been applied to concrete.	Hysteresis in load-distance curve on insertion and removal on indenter requires interpretation. Extremely flat surface is needed. Thus, the technique may be difficult to apply to concrete where preparation of such surfaces is very difficult and phases pull-out occurs during polishing. Resolution is probably limited to around 1 mm.
Laser holographic Interferometry	• 0.25 μm	A laser beam is scanned over a flat specimen before and after loading and the fringe patterns in the two conditions are overlaid, producing an interferogram and revealing any cracks as surface displacements[34].	Although holograms provide a large amount of information which can be quantified, it is difficult to use the information quantitatively.

44

---

[32]E. Sellevold, and D. Bager (1980) *Proceedings of the 7th International Congress on the Chemistry of Cement, Paris*, p. 394;
C. le Sage de Fontenay, and E. Sellevold (1980) In *Durability of Building Materials and Components*, STP 691, P. Serenda and G. Litvan, Ed., ASTM, Philadelphia, p. 425;
L. Homshaw (1980) *Journal of Thermal Analysis*, **19:** 215.
[33]M.J. Setzer (1987) *Proceedings of the Materials Research Society*, Vol. 85, MRS, Pittsburgh, p.307.
[34]S.P. Shah, and C. Ouyang (1989) In *Materials Science of Concrete and Cement* (J. Skalny, Ed.) Vol III, The American Ceramic Society, Westerville, Ohio, p. 243.

APPENDIX C (CONT'D): INDIRECT TECHNIQUES

Technique	Resolution	Advantages	Disadvantages
Moiré interferometry	• resolution depends on grating size	A standard technique which has been applied to concrete is using an interference grating on the surface of the specimen to study cracking[35].	The main problem is the difficulty transferring the grating to the surface of the concrete.
Photoelasticity		A photoelastic coating glued onto the specimen surface from which light is reflected during deformation can be used to study cracks[2]. A brittle coating (unpolymerized Araldite) is appropriate to study concrete.	Coatings have to be sufficiently thin (0.5– 3.0 mm) to minimize effects on the specimen being studied

---

[35]A.K. Maji (1995) *Advances in Cement Based Materials*, **2**: 201.

APPENDIX D: DERIVATIONS

These derivations are based on a simple application of thermodynamics. They ignore changes in surface energies with temperature, and do not consider the reduction in the entropy of water as the pore liquid becomes dominated by the "structured" water at the gel surface.

Freezing point suppression (eq 6)

Assume that only the liquid phase is under tension. At equilibrium:

$$\mu_l = \mu_s \tag{D1}$$

or

$$H_l - TS_l - V_l\Delta P = H_s - TS_s \tag{D2}$$

where μ is the chemical potential, and H, S and V are molar enthalpy, molar entropy and molar volume, respectively. T is absolute temperature and the subscripts l and s denote liquid and solid, respectively. Assuming that H is relatively independent of temperature near $T_o = 273$ K and writing

$$H_l = H_s + L \tag{D3}$$

where L is the molar heat of fusion, and writing

$$S_l = S_s + \frac{L}{T_o} \tag{D4}$$

then for equations D2, D3, and D4 and eq 5 (text):

$$\frac{T}{T_o} = \frac{1 - 2V_l\gamma_{lv}\cos\phi}{rL} \tag{D5}$$

or

$$\Delta T = T - T_o = \frac{-2T_o V_l\gamma_{lv}\cos\phi}{rL} \tag{D6}$$

where T is the equilibrium freezing point of water within a pore of radius r and ΔT is the freezing point suppression.

Pressure melting temperature, T_p (eq 8)

Assume that only the solid phase is under compression. At equilibrium,

$$\mu_l = \mu_s \tag{D1}$$

or

$$H_l - T_p S_l = H_s - T_p S_s + V_s\Delta P_p \tag{D7}$$

Again, let $H_l = H_s + L$ and let $S_l = S_s + L / T_o$. Then

$$\frac{T_p}{T_o} = 1 - \frac{V_s\Delta P_p}{L}$$

or

$$T_{\mathrm{p}} = T_{\mathrm{o}}\left(1 - \frac{V_{\mathrm{s}}\Delta P_{\mathrm{p}}}{L}\right) \tag{D8}$$

Writing

$$\Delta P_{\mathrm{p}} = 2\gamma_{\mathrm{sl}}\left(\frac{1}{r} - \frac{1}{R}\right) \tag{D9}$$

Then

$$T_{\mathrm{p}} = T_{\mathrm{o}}\left[1 - \frac{2V_{\mathrm{s}}\gamma_{\mathrm{sl}}}{L}\left(\frac{1}{r} - \frac{1}{R}\right)\right] \tag{D10}$$

For $R \gg r$, then

$$T_{\mathrm{p}} = T_{\mathrm{o}}\left[1 - \frac{2V_{\mathrm{s}}\gamma_{\mathrm{sl}}}{rL}\right] \tag{D11}$$

similar to eq D6.

REPORT DOCUMENTATION PAGE

Form Approved
OMB No. 0704-0188

1. AGENCY USE ONLY (Leave blank)	2. REPORT DATE April 1998	3. REPORT TYPE AND DATES COVERED

4. TITLE AND SUBTITLE
Ice Damage to Concrete

5. FUNDING NUMBERS

6. AUTHORS
Erland M. Schulson

7. PERFORMING ORGANIZATION NAME(S) AND ADDRESS(ES)

Dartmouth College
Hanover, New Hampshire 03755

8. PERFORMING ORGANIZATION REPORT NUMBER
Special Report 98-6

9. SPONSORING/MONITORING AGENCY NAME(S) AND ADDRESS(ES)

U.S. Army Cold Regions Research and
  Engineering Laboratory
72 Lyme Road
Hanover, New Hampshire 03755

U.S. Department of Transportation
Federal Highway Administration
Washington, DC 20590

10. SPONSORING/MONITORING AGENCY REPORT NUMBER

11. SUPPLEMENTARY NOTES

12a. DISTRIBUTION/AVAILABILITY STATEMENT
Approved for public release; distribution is unlimited.
Available from NTIS, Springfield, Virginia 22161

12b. DISTRIBUTION CODE

13. ABSTRACT (*Maximum 200 words*)

Concrete is a porous material. When saturated with water and then cooled to below 0°C, it cracks internally. Upon repeated freezing and thawing, the cracks grow, interact, and lead eventually to macroscopic degradation, termed ice damage. This report reviews the phenomenon and considers the underlying mechanisms. New explanations are given for the deleterious effect of deicer salts and for the beneficial effect of entrained air.

14. SUBJECT TERMS		15. NUMBER OF PAGES 55
Concrete Deicing salts	Ice damage Portland cement	
		16. PRICE CODE

17. SECURITY CLASSIFICATION OF REPORT	18. SECURITY CLASSIFICATION OF THIS PAGE	19. SECURITY CLASSIFICATION OF ABSTRACT	20. LIMITATION OF ABSTRACT
UNCLASSIFIED	UNCLASSIFIED	UNCLASSIFIED	UL